

The route to prolonged residence time at the histamine H receptor: growing from desloratadine to rupatadine

Reggie Bosma, Zhiyong Wang, Albert J. Kooistra, Nick Bushby, Sebastiaan Kuhne, Jelle van den Bor, Michael J. Waring, Chris de Graaf, Iwan J. P. De Esch, Henry F. Vischer, Robert J Sheppard, Maikel Wijtmans, and Rob Leurs

J. Med. Chem., **Just Accepted Manuscript** • DOI: 10.1021/acs.jmedchem.9b00447 • Publication Date (Web): 20 Jun 2019

Downloaded from <http://pubs.acs.org> on June 24, 2019

Just Accepted

“Just Accepted” manuscripts have been peer-reviewed and accepted for publication. They are posted online prior to technical editing, formatting for publication and author proofing. The American Chemical Society provides “Just Accepted” as a service to the research community to expedite the dissemination of scientific material as soon as possible after acceptance. “Just Accepted” manuscripts appear in full in PDF format accompanied by an HTML abstract. “Just Accepted” manuscripts have been fully peer reviewed, but should not be considered the official version of record. They are citable by the Digital Object Identifier (DOI®). “Just Accepted” is an optional service offered to authors. Therefore, the “Just Accepted” Web site may not include all articles that will be published in the journal. After a manuscript is technically edited and formatted, it will be removed from the “Just Accepted” Web site and published as an ASAP article. Note that technical editing may introduce minor changes to the manuscript text and/or graphics which could affect content, and all legal disclaimers and ethical guidelines that apply to the journal pertain. ACS cannot be held responsible for errors or consequences arising from the use of information contained in these “Just Accepted” manuscripts.

1
2
3 **The route to prolonged residence time at the histamine H₁ receptor: growing from desloratadine to**
4
5 **rupatadine**
6

7 Reggie Bosma^{a1}, Zhiyong Wang^{a1}, Albert J. Kooistra^a, Nick Bushby^c, Sebastiaan Kuhne^a, Jelle van den Bor^a,
8
9 Michael J. Waring^d, Chris de Graaf^a, Iwan J. de Esch^a, Henry F. Vischer^a, Robert J. Sheppard^b, Maikel
10
11 Wijtman^a and Rob Leurs^{a*}
12
13

14
15
16
17 ^a Amsterdam Institute for Molecules, Medicines and Systems; Division of Medicinal Chemistry, Faculty of
18
19 Science, VU University Amsterdam, De Boelelaan 1083, 1081 HV, Amsterdam, the Netherlands.

20
21 ^b Medicinal Chemistry, Research and Early Development, Cardiovascular, Renal and Metabolism,
22
23 BioPharmaceuticals R&D, AstraZeneca, Gothenburg, 431 50, Sweden.

24
25 ^c Operations, BioPharmaceuticals R&D, AstraZeneca, Alderley Park, Macclesfield, SK10 4TG, United
26
27 Kingdom.

28
29
30 ^d Medicinal Chemistry, Research and Early Development, Oncology R&D, AstraZeneca, Alderley Park,
31
32 Macclesfield, SK10 4TG, United Kingdom.

33
34 ¹Authors contributed equally to this manuscript.

35
36
37 *Corresponding author: r.leurs@vu.nl
38
39
40

41 **Abstract**
42

43 Drug-target binding kinetics are an important predictor of *in vivo* drug efficacy, yet the relationship
44
45 between ligand structures and their binding kinetics is often poorly understood. We show that both
46
47 rupertadine (**1**) and desloratadine (**2**) have a long residence time at the histamine H₁ receptor (H₁R).
48
49 Through development of a [³H]levocetirizine radiolabel, we find that the residence time of **1** exceeds
50
51 that of **2** more than 10-fold. This was further explored with 22 synthesized rupertadine and desloratadine
52
53 analogs. Methylene-linked cycloaliphatic or beta-branched substitutions of desloratadine increase the
54
55
56
57
58
59
60

1
2
3 residence time at the H₁R, conveying a longer duration of receptor antagonism. However, cycloaliphatic
4
5 substituents directly attached to the piperidine amine (i.e. lacking the spacer) have decreased binding
6
7 affinity and residence time compared to their methylene-linked structural analogs. Guided by docking
8
9 studies, steric constraints within the binding pocket are hypothesized to explain the observed
10
11 differences in affinity and binding kinetics between analogs.
12
13
14
15
16
17
18
19
20
21
22
23
24
25
26
27
28
29
30
31
32
33
34
35
36
37
38
39
40
41
42
43
44
45
46
47
48
49
50
51
52
53
54
55
56
57
58
59
60

Introduction

Drugs have to bind a therapeutically relevant target to exhibit a biological effect and, as such, target binding is well characterized during the development process of many drugs. The binding affinity is an often-used parameter to measure drug binding to a target (quantified as K_D or K_i values), implicitly assuming ligand binding occurs under equilibrium conditions. However, drug pharmacodynamics can also be characterized by the drug-target binding kinetics, which provide important details about the mechanism of target binding, unexplained by solely the binding affinity.¹⁻³ The drug-target residence time, which is a measure for the lifetime of a drug-target complex, is currently discussed as one of the important contributors to the biological efficacy of drugs *in vivo*.³⁻¹⁰ It has been postulated that a suitably long drug-target residence time might increase the therapeutic window *in vivo* when clearance of the drug is faster than the dissociation of the drug from the receptor.^{11,12} In such cases, drug action would last longer than the presence of free drug plasma concentrations (i.e. *hysteresis*). Thus, duration of therapeutic action may not only depend on drug absorption, distribution, metabolism, and excretion (and the nature of its metabolites), but can also be a direct effect of prolonged target binding.¹³⁻¹⁵

As the target of 33% of all small molecule drugs, the G protein-coupled receptors (GPCRs) are an important class of proteins in drug discovery.¹⁶ The histamine H_1 receptor (H_1R) is an archetypical GPCR and is successfully targeted by antagonists for the treatment of, for example, allergic disorders.¹⁷ A long duration of action has been observed *in vivo* for second generation H_1R antagonists, like levocetirizine and fexofenadine, which have a long residence time at the H_1R .^{18,19} Hysteresis was indeed observed for levocetirizine and fexofenadine.¹⁸⁻²⁰ A strong hysteresis of H_1R antagonism has also been shown for rupatadine (**1**), which antagonizes the histamine-induced flare response up to 72 hours after oral administration, whereas plasma levels could only be detected up to 12 hours after administration.²¹ This might be explained by metabolism of rupatadine to metabolites such as desloratadine (**2**), which is a known antihistamine itself with a long H_1R residence time (>1 h) and a long plasma half-life *in vivo*

(human).^{19,21–27} Yet, a potentially long drug-target residence time of rupatadine may also be a crucial contributing factor to its observed long duration of action.

Here, we report the measurement of the residence times of rupatadine and desloratadine at the H₁R. It was shown that rupatadine has a ≥ 10 fold longer residence time at the H₁R, relative to desloratadine. As a consequence, rupatadine completely antagonized the histamine-induced calcium mobilization in HeLa cells for > 2 hrs after removal of unbound antagonist, whereas inspected under the same conditions, desloratadine allowed a time-dependent gradual recovery of the histamine-induced response. To understand the structure-kinetics relationship (SKR) for rupatadine and desloratadine in more detail, the binding kinetics at the H₁R were characterized for newly synthesized analogs (**3-24**) that retain the core scaffold of **1** and **2** but contain a diverse set of aromatic and aliphatic N-substituents on the piperidine ring. It was shown that relatively small aliphatic N-substitutions were sufficient for a prolonged H₁R residence time compared to desloratadine, unless this was negated by steric interference in the binding pocket.

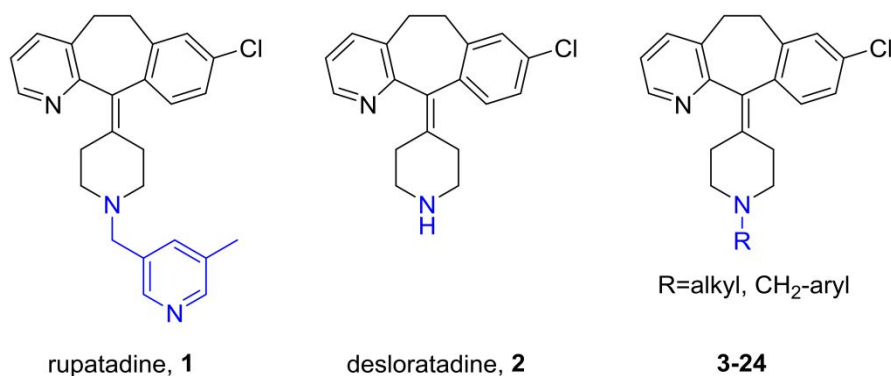


Figure 1-Structures of the investigated H₁R antagonists and synthesized structural analogs.

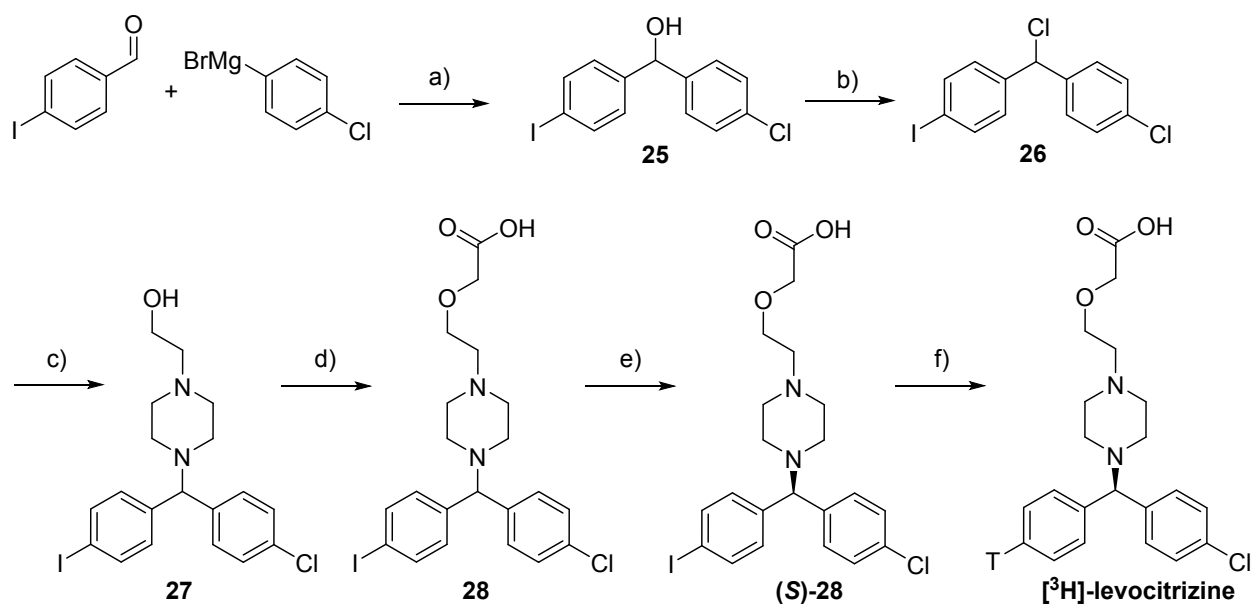
Results

Binding properties of rupatadine and desloratadine at the H₁R.

Based on the long duration of action of rupatadine *in vivo*,²¹ we hypothesized that it would exhibit a long residence time at the H₁R. Therefore, binding of rupatadine and its structural analog desloratadine to

1
2
3 the human H₁R was investigated, initially using [³H]mepyramine and standardized competition binding
4 experiments.²⁶ The H₁R binding affinity of desloratadine (pK_i 9.1 ± 0.1) determined in these experiments
5 was consistent with previously reported affinity values (pK_i = 8.8 – 10^{24–26}). Rupatadine (pK_i 8.4 ± 0.1)
6 was shown to have a five-fold lower binding affinity for the H₁R than desloratadine. To the best of our
7 knowledge, the binding affinity of rupatadine on the human H₁R has not been reported in the literature.
8 Its H₁R activity on guinea pig ileum is known, as well as that for a series of derivatives.²⁸
9
10 Competitive association experiments were subsequently performed to examine the binding kinetics of
11 rupatadine and desloratadine at the H₁R. Initially, [³H]mepyramine was selected as radioligand and
12 experiments were performed at 25°C with an 80 min incubation time, in the manner described
13 previously.²⁶ A clear initial overshoot in [³H]mepyramine binding was observed for both unlabeled
14 ligands (Figure 2A), which is indicative of the long residence times of the unlabeled ligands relative to
15 [³H]mepyramine.^{29,30} However, since the binding curves of rupatadine and desloratadine showed similar
16 overshoot patterns, it was difficult to discern differences in their binding kinetics using the Motulsky-
17 Mahan analysis.³⁰ Desloratadine was found to have a residence time of 190 ± 40 min (similar to that
18 reported in the literature^{25,26}), but for rupatadine the k_{off} value (and thus the residence time) could not
19 be accurately constrained by the model. To overcome this limitation, it was speculated that the
20 residence times of desloratadine and rupatadine at the H₁R might be better discriminated using a
21 radioligand with a longer residence time, and one more closely matched to desloratadine and
22 rupatadine than mepyramine. With this in mind, levocetirizine was considered a better alternative as it
23 is known to have a 100-fold longer residence time at the H₁R than mepyramine.²⁵ Radiolabeled
24 levocetirizine has previously been disclosed but without synthetic details for its preparation.²⁵ The
25 radiolabel was prepared by us using a six-step sequence progressing through intermediates **25-28**.
26 Separation of the enantiomers of **28**, followed by Pd-catalyzed dehalotritiation of the corresponding aryl
27
28
29
30
31
32
33
34
35
36
37
38
39
40
41
42
43
44
45
46
47
48
49
50
51
52
53
54
55
56
57
58
59
60

iodide delivered the ligand with a specific activity of 956 GBq mmol⁻¹ (Scheme 1, and supplementary information).



Scheme 1 - Synthesis of [³H]levocitrizine. Key: (a) Et₂O, 0 °C to r.t., 16 h, 88 %; (b) SOCl₂, DCM, r.t., 20 h, 95 %; (c) 2-(piperazin-1-yl)ethanol, PhMe, 80 °C, 20 h, 21 %; (d) (1) KOH, DMF, 0 °C, 90 min; (2) sodium 2-chloroacetate, DMF, 0 °C, 3 h, 57 %; (e) Chiral separation; (f) T₂, Pd/C (10 %), Et₃N, EtOH.

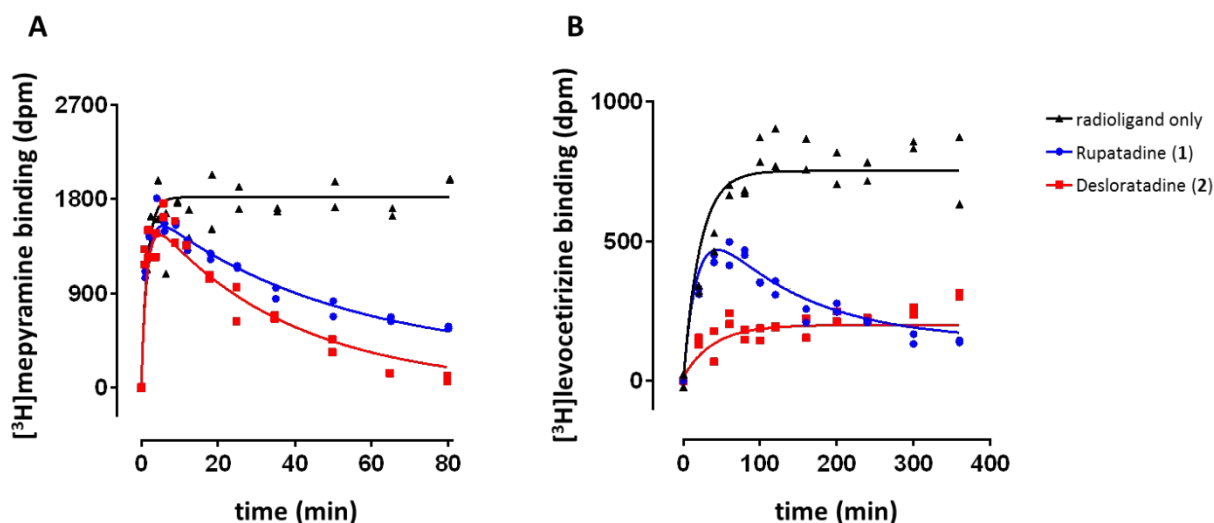


Figure 2 – Radioligand association binding when co-incubated with rupertadine and desloratadine. A homogenate of HEK293T cells expressing the H₁R was incubated with: (A) [³H]mepyramine (3.8 nM) alone, or in the presence of either rupertadine (130 nM) or desloratadine (4 nM); or (B), - [³H]levocitrizine (6.6 nM) alone, or in the presence of either rupertadine (6 nM) or

desloratadine (0.7 nM). Representative graphs of 3 experiments are shown depicting individual measurements with duplicate values per time point.

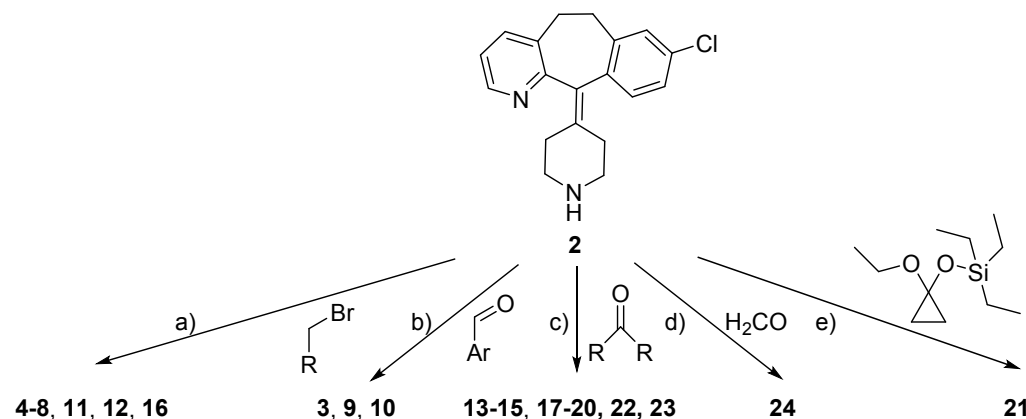
[³H]levocetirizine was then employed in competitive association experiments to characterize the binding kinetics of rupatadine and desloratadine using an incubation time of 6 hours (to ensure a steady state in [³H]levocetirizine binding). In the presence of desloratadine, [³H]levocetirizine binding to the H₁R increased gradually over time, whereas in the presence of rupatadine a clear initial overshoot in [³H]levocetirizine binding was observed (Figure 2). Based on these curve shapes, it is clear that rupatadine has a longer residence time on the H₁R than desloratadine. Fitting the data to the Motulsky-Mahan model³⁰ did not result in a precise fit of the k_{off} values, but indicated the k_{off} of desloratadine at the H₁R to be $> 0.03 \text{ min}^{-1}$ (P = 95% in all 3 experiments) corresponding to a residence time of $< 33 \text{ min}$. In the case of rupatadine, the k_{off} value at the H₁R is $< 0.0033 \text{ min}^{-1}$ (P = 95% in all 3 experiments), which corresponds to a residence time of $> 300 \text{ min}$. Thus, rupatadine has a very long residence time at the H₁R, which is at least 10-fold longer than observed for desloratadine.

Design and synthesis of rupatadine analogs at the H₁R

To identify the structural features that drive the longer residence time of rupatadine as compared to desloratadine at the H₁R, various analogs were synthesized and pharmacologically characterized.

Rupatadine contains a 5-methylpyridin-3-yl group connected through a methylene to the basic amine of desloratadine (Figure 1). To study the SKR, we synthesized analogs with the methyl group on different positions of the pyridine ring (**3-5**), and the pyridine analog without the methyl group (**6**). Two positional isomers of **6** (**7, 8**), and two pyrimidines (**9-10**) were also prepared. Additionally, the pyridine ring of rupatadine was replaced by a phenyl ring with (**11**), or without (**12**), a 3-methyl group. Finally, to gradually bridge the transition to **2**, a set of analogs was synthesized in which the basic amine of desloratadine was substituted with a range of alkyl groups (**13-24**), varying in size, level of

constrainment and point of attachment (with or without the one-carbon spacer). Of these, only **3-8**, **12**, **23** and **24** have been reported before.^{28,31-34}



Scheme 2 — Synthesis of rupatidine analogs. Key: (a) K_2CO_3 , DMF, rt, 18 h, 36–86%; (b) $NaBH(OAc)_3$, DCE, rt, 14 h, 64–88%; (c) $NaBH(OAc)_3$, DCE, rt, 14 h, 52–71%; (d) $NaBH(OAc)_3$, MeOH, DCM, AcOH, rt, 1.5 h, 60% as fumarate salt; (e) $NaBH(OAc)_3$, AcOH, DCM, rt, 48 h, 17%.

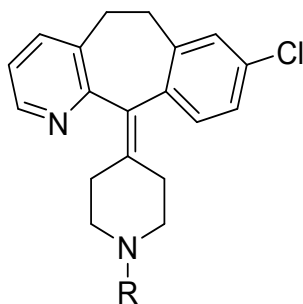
All rupatidine analogues were efficiently obtained in one step from commercially available desloratidine (**2**), as depicted in Scheme 2. Compounds **4-8**, **11-12** and **16** were obtained *via* nucleophilic substitution of the corresponding alkyl bromides in moderate to good yields (36-86%). Reductive alkylation of **2** with different aromatic aldehydes afforded **3**, **9** and **10** (64-88% yield). Compounds **13-15**, **17-20**, **22** and **23** were synthesized by reductive alkylation using aliphatic carbonyl compounds in acceptable to good yields (52-71%). Methyl-derivative **24** was obtained as the fumarate salt from aqueous formaldehyde and $NaBH(OAc)_3$ in 60% yield. Attempted synthesis of cyclopropyl-substituted analogue **21** via alkylation of **2** with cyclopropylbromide failed. However, reductive alkylation of **2** with (1-ethoxycyclopropoxy)triethylsilane delivered the desired product, albeit in low isolated yield (17%).³⁵

Pharmacological characterization

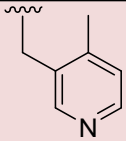
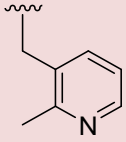
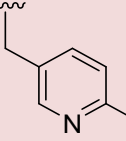
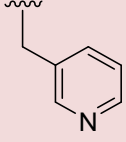
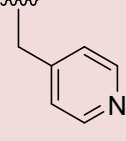
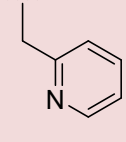
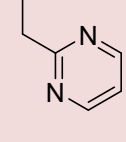
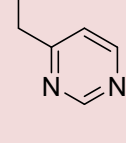
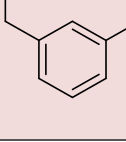
H_1R binding affinity

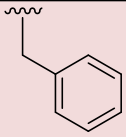
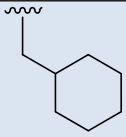
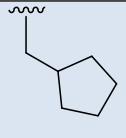
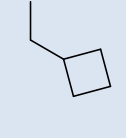
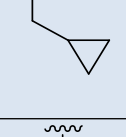
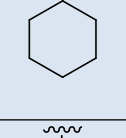
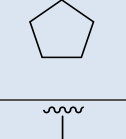
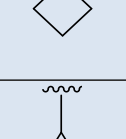
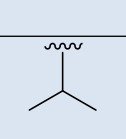
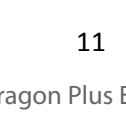
1
2
3 All rupatadine analogs containing an aromatic group (**3-12**) had comparable binding affinities at the H₁R
4 (pK_i 7.9 – 8.5) as rupatadine, which were 4-16 fold lower than the binding affinity of desloratadine (pK_i =
5 9.1). Substituting the benzene of **12** for a cyclohexane (**13**) did not affect the binding affinity (<2-fold).
6
7
8 However, substituting the benzene of **12** for smaller methylene-linked cycloaliphatic N-substituents (**14**,
9
10
11
12
13
14
15
16
17
18
19
20
21
22
23
24
25
26
27
28
29
30
31
32
33
34
35
36
37
38
39
40
41
42
43
44
45
46
47
48
49
50
51
52
53
54
55
56
57
58
59
60

Table 1 – H₁R binding of rupatadine and desloratadine analogs. Binding affinity (pK_i) values were determined by competition binding experiments using [³H]mepyramine and KRI-values were determined by dual-point competition association experiments using [³H]levocetirizine. Depicted values represent the mean ± SEM of ≥ 3 experiments.



Cmpd#	Name	R	pK _i	KRI
1	rupatadine		8.4 ± 0.1	2.3 ± 0.2
2	desloratadine		9.1 ± 0.1	0.82 ± 0.04

1 2 3 4 5 6 7 8 9 10 11 12 13 14 15 16 17 18 19 20 21 22 23 24 25 26 27 28 29 30 31 32 33 34 35 36 37 38 39 40 41 42 43 44 45 46 47 48 49 50 51 52 53 54 55 56 57 58 59 60	3^b	VUF15718		7.89 ± 0.05	2.4 ± 0.4
	4^b	VUF15769		8.05 ± 0.04	5.4 ± 3.5
	5^b	VUF15717		8.12 ± 0.04	5.8 ± 1.7
	6^b	VUF15713		8.3 ± 0.1	4.3 ± 1.5
	7^b	VUF15712		8.1 ± 0.3	3.8 ± 0.5
	8^b	VUF15714		8.5 ± 0.1	2.4 ± 0.5
	9	VUF15877		8.5 ± 0.1	1.3 ± 0.1
	10	VUF15886		8.3 ± 0.1	1.3 ± 0.1
	11	VUF15716		8.1 ± 0.1	3.3 ± 0.9

12^b	VUF15715		8.4 ± 0.1	1.9 ± 0.5
13	VUF16138		8.6 ± 0.2	1.9 ± 0.3
14	VUF16140		8.9 ± 0.2	1.6 ± 0.2
15	VUF16141		8.75 ± 0.05	1.4 ± 0.2
16	VUF16137		9.1 ± 0.2	1.2 ± 0.1
17	VUF16139		9.2 ± 0.1	1.7 ± 0.1
18	VUF16136		7.7 ± 0.1	0.9 ± 0.1
19	VUF16135		8.4 ± 0.2	0.7 ± 0.1
20	VUF16142		8.67 ± 0.04	0.81 ± 0.04
21	VUF 16219		8.5 ± 0.1	0.76 ± 0.03
22	VUF16143		9.0 ± 0.1	1.1 ± 0.3

23^b	VUF16144		9.38 ± 0.03	1.2 ± 0.1
24^{a,b}	VUF15007		9.4 ± 0.1	1.1 ± 0.2

^a fumarate salt. ^b Previously reported (see text for references).

Analysis of binding kinetics

To explore the relative residence time of all analogs, a dual-point competition association was performed to determine the kinetic rate index (KRI).²⁹ This methodology is based on the initial overshoot in radioligand binding when co-incubated with an unlabeled ligand, which is an indicator of a relatively long residence time of the unlabeled ligand compared to that of the radioligand (Figure 2). The overshoot is quantified by measuring the radioligand binding at two time points. The ratio in [³H]levocetirizine binding at both time points (1 and 6 hours) is > 1 for unlabeled ligands that cause an initial overshoot in [³H]levocetirizine binding and hence have a relatively long residence time compared to [³H]levocetirizine. Using this assay setup, a KRI value of 0.9 ± 0.1 was obtained for unlabeled levocetirizine, demonstrating that, as expected, it has a residence time essentially the same as the radioligand. Desloratadine does not cause an initial overshoot in [³H]levocetirizine binding (Figure 2B) and has a KRI value of 0.82 ± 0.04 . In contrast, rupatadine binds the H₁R with a much longer residence time (Figure 2B), which is indeed reflected by its KRI value of 2.3 ± 0.2 (Table 1). The KRI values for all analogs are given in Table 1. All analogs with an aromatic substituent (**3-12**) show KRI values > 1, indicative of a consistently long residence time at the H₁R (Table 1). More notably, among the analogs with aliphatic substitutions on the piperidine ring (**1,2,13-24**), large differences in the KRI values were observed (Figure 3). This intriguing SKR in the aliphatic series, in combination with the lack thereof in the aromatic series, led us to focus on the former series.

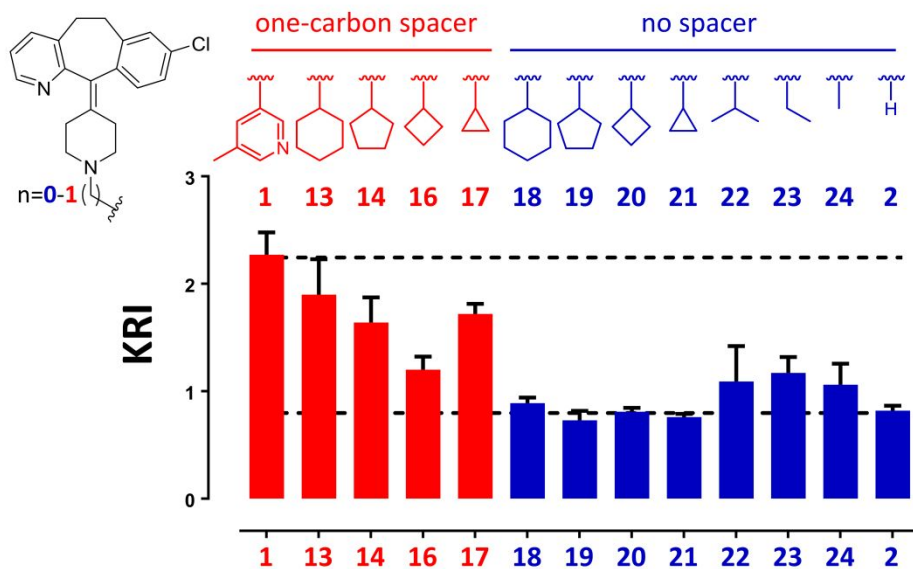


Figure 3– Aliphatic substituents on the basic amine of desloratadine cause differential binding kinetics at the H₁R. A homogenate of HEK293T cells expressing the H₁R was incubated with [³H]levocetirizine and the respective ligands. Binding of [³H]levocetirizine was determined after 1 h and 6 h and the KRI value was determined as the ratio in [³H]levocetirizine binding at both time points (6 h/1h). The bars depict the mean and SEM of ≥ 3 experiments. The upper and lower dotted lines represent the KRI of reference ligands **1** and **2**, respectively.

Analogues with cycloaliphatic groups and a one-carbon spacer (**13**, **14**, **16** and **17**) show high KRI values, also indicating a long residence time on the H₁R. However, structural analogues with the same cycloaliphatic group without the one-carbon spacer (**18-21**) show similar KRI values to desloratadine, indicative of a shorter residence time at the H₁R. Additionally, analogues with small acyclic aliphatic substituents (**22-24**) had an average KRI value slightly larger than 1, implying an increased residence time at the H₁R compared to desloratadine. Correlation between affinity and residence time parameters of GPCR ligands and physicochemical properties of the ligands has been investigated, including affinities for H₁R receptor antagonists,^{36,37} by various research groups.³⁸⁻⁴⁵ Therefore, we investigated whether correlations exist between our pK_i/KRI values and key physicochemical parameters (log D7.4, Polar Surface Area (PSA), van der Waals volume, pK_a value of the conjugate acid of the piperidine nitrogen atom). However, Supplementary Fig 1, Table 1 and Table 2 show that no strong correlations are evident.

Duration of functional H₁R-antagonism

Since large differences were observed in the KRI values of the aliphatic rupatadine analogs, these differences were explored in more detail by measuring the kinetics of functional H₁R-antagonism following a pre-incubation with the selected analogs of interest. The functional recovery time of the H₁R was previously shown to be correlated with the residence time of antagonists.⁴⁶ As such, HeLa cells, with endogenous expression of the H₁R, were pre-incubated with 10 times the K_i-concentration of the respective compound. Unbound ligands were then depleted by washing the cells, which were subsequently stimulated after different incubation times with 10 μM histamine. The intracellular calcium mobilization following administration of histamine was determined with the calcium sensitive fluorescent-dye (Fluo4 NW).

Pre-incubating HeLa cells with desloratadine, which has a low KRI value (<1), resulted in functional recovery of the H₁R over time (Figure 4A; Supplementary Table 1). However, cells pre-treated with rupatadine were completely unresponsive to histamine, for at least for 2 hours after removing unbound rupatadine, suggesting very persistent target-engagement by rupatadine. In Figure 4B, the functional recovery of the H₁R is compared after pre-treating the cells with analogs containing cycloaliphatic N-substituents on the piperidine with or without a one-carbon spacer. Analogues with a one-carbon spacer (**14**, **16** and **17**) completely abolished the histamine-induced calcium response for at least 2 hours, similarly to rupatadine. In contrast, and in line with the measured KRI values, removing the one-carbon

spacer (**19-21**), allowed a relatively fast functional recovery of the histamine response.

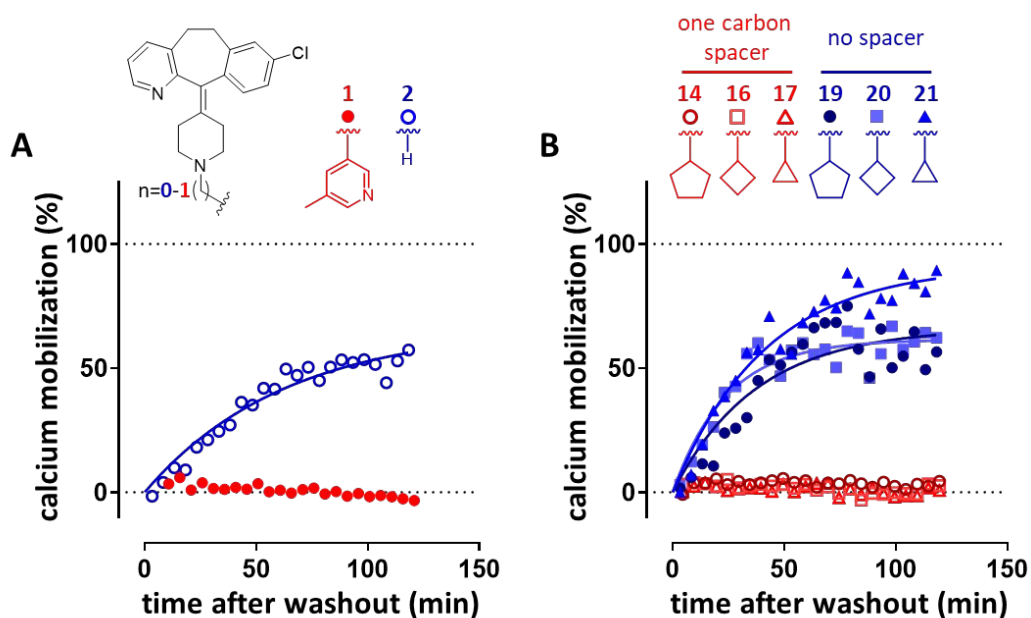


Figure 4– Functional recovery of histamine-induced calcium mobilization after a pre-incubation with ligands that bind the H₁R. HeLa cells were pre-incubated for 18-20 h with the respective H₁R-ligand, reaching stable and high ($\pm 90\%$) occupancy of the endogenously expressed H₁R. Cells were then labeled with Fluo4NW in the presence of the respective ligands for 1 h. All excess Fluo4NW and unbound ligands were removed by wash steps and cells were subsequently stimulated with histamine (10^{-5} M) after different incubation times. Representative graphs of ≥ 3 experiments are shown, which depict the normalized calcium mobilization that was measured at each time point after washout. **(A)** Cells were pre-incubated with the reference H₁R antagonists: rupatadine (**1**) and desloratadine (**2**). **(B)** Cells were pre-incubated with compounds having various cycloalkyl substituents on the basic amine with (**14, 16, 17**) or without (**19, 20, 21**) a one-carbon spacer.

The differences in the combined kinetic/affinity binding profiles of the compounds were further explored on a structural level with docking studies. Using the X-ray crystal structure of the H₁R with the structurally-related ligand doxepin bound,⁴⁷ reference compounds desloratadine, rupatadine, as well as all analogs (**3-24**) were docked using PLANTS.⁴⁸ Figure 5 shows the postulated binding modes of desloratadine, rupatadine, and the representative pair **14/19**, in comparison to the binding mode of the co-crystallized ligand doxepin. Desloratadine likely adopts a similar binding pose to that observed for doxepin in the H₁R crystal structure (Figure 5A). Rupatadine was also found to adopt a similar binding

mode to doxepin, but its (5-methylpyridin-3-yl)methyl moiety targets an additional area of the H₁R binding pocket towards the extracellular vestibule (Figure 5B). Since the available space in the H₁R binding pocket next to the amine-binding region is limited by I454^{7.39} and Y458^{7.43}, it is postulated that the cyclopentyl substituent of **19** encounters greater steric hindrance than the cyclopentylmethyl substituent of **14** (Figure 5C), in line with the altered H₁R binding characteristics of **19**. (Figure 3 and Figure 4B). This steric hindrance results in a tilted binding mode compared to desloratadine, which is not observed for optimal binding of analogs with a methylene spacer between the desloratadine scaffold and the cyclopentyl group (**14**, Figure 5D). The spacer allows the aliphatic group to turn towards the extracellular vestibule (in the direction of H450^{7.35}) where more room is available, possibly preventing a steric clash with I454^{7.39} and Y458^{7.43} (Figure 5D).

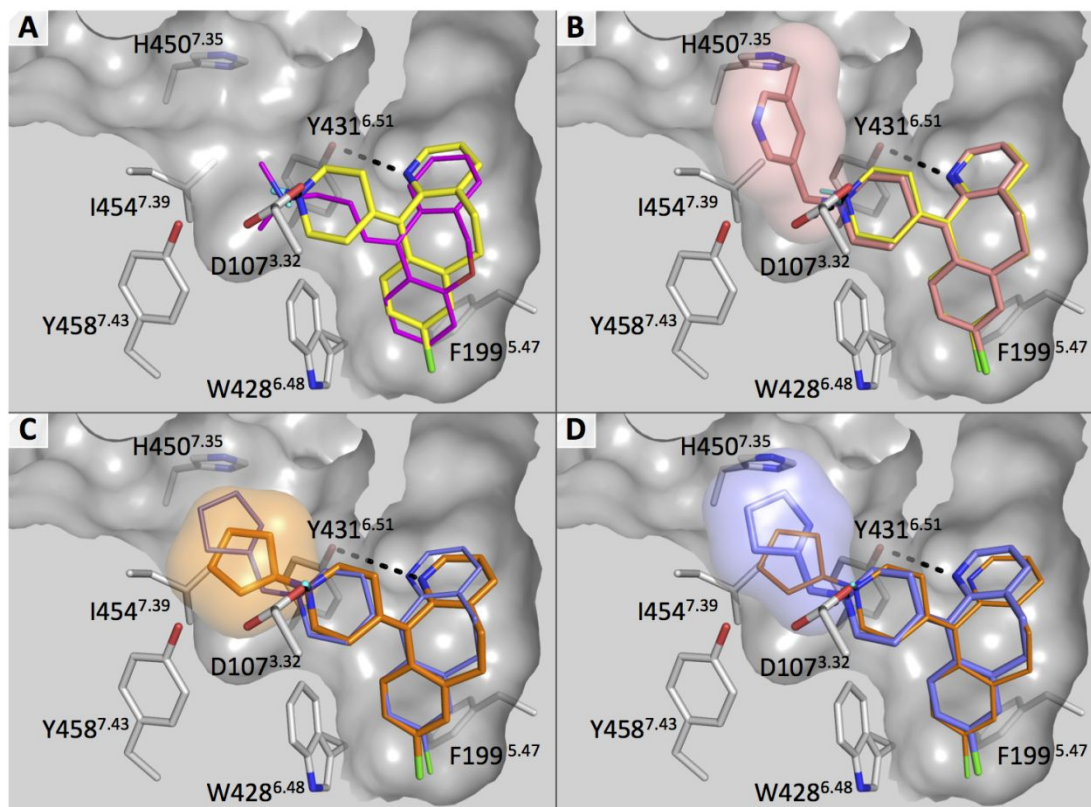


Figure 5– Proposed binding modes of A) Desloratadine (yellow), B) Rupatadine (salmon), and C/D) compound **19** (orange) in comparison to compound **14** (blue) based on docking⁴⁸ into the crystal structure (PDB-code 3RZE⁴⁷) of the H₁R in complex with Doxepin (magenta, see A). The clipped molecular surface of H₁R highlights the limited space for growing from the amine

of desloratadine due to I454^{7,39} and Y458^{7,43}. To highlight the fit of the substituents of rupatadine (**2**, **B**), **19** (**C**), and **14** (**D**) compared to desloratadine in the H₁R binding pocket, they are shown as transparent surfaces.

Discussion and conclusions

A long drug-target residence time has been postulated to benefit the *in vivo* efficacy of several drugs for a broad number of drug targets, among which is the H₁R.^{3,4,7,49,50} Affinity-based optimization of drug binding does not necessarily reflect differences in target residence time,^{51,52} and a discrepancy between affinity and residence time at the H₁R was previously described. Moreover, in the case of ligands that do not reach a binding equilibrium within the time-frame of a binding experiment, i.e. ligands with a very slow off rate like rupatadine, the pK_i will be underestimated.⁵³ The drug-target residence time can therefore provide additional information for the optimization of drugs that would be lost by focusing on only the binding affinity. Since the residence time is not routinely incorporated in drug development, design strategies for optimizing the drug-target residence time of lead compounds are not widely available. Since rupatadine is shown here to have a much longer residence time at the H₁R than its close structural analog desloratadine, despite a reduced binding affinity, it provides an opportunity for a detailed investigation of the SKR for this GPCR. Towards this end, we synthesized [³H]levocetirizine which proved to be a useful tool to map the differences in the KRIs between the two antihistamines. It was therefore employed to determine the relative residence times of structural analogs **3-24**. Several analogs of rupatadine were designed to replace the (5-methylpyridin-3-yl)methyl group with other aromatic moieties (**3-12**). Interestingly, the K_i values of **3-12** are within 4-fold of the K_i value of rupatadine. Additionally, all aromatic analogs have a long apparent residence time, as is reflected by the KRI > 1. Removing the aromatic character of the functional group of **12** by replacing it with a cyclohexyl group (**13**) does not affect the observed H₁R binding properties either. Hence, the strong effect on the residence time by the (5-methylpyridin-3-yl)methyl group of rupatadine (compared to desloratadine)

1
2
3 cannot be explained by the aromatic character, nor by the pyridine nitrogen atom and the methyl
4
5 substituent.
6

7 To further probe the SKR between rupatadine and desloratadine, a series of analogs was characterized
8
9 that had different aliphatic substituents on the piperidine group (**13-24**). Strikingly, most aliphatic
10
11 moieties afford an increase in the KRI compared to desloratadine, whereas the binding affinity remains
12
13 similar or even decreases. For example, **13-15** contain relatively large aliphatic substituents (≥ 6 -
14
15 carbons) and have a slightly reduced binding affinity (pK_i 8.6 – 8.9) and a high KRI (> 1.4) as compared to
16
17 desloratadine. Moreover, analogs with small (≤ 3 -carbons) acyclic aliphatic substituents (**22-24**) have a
18
19 similar binding affinity but still a slightly higher KRI compared to desloratadine. This suggests that
20
21 growing an aliphatic group from the piperidine increases the residence time at the H_1R . This trend is
22
23 disrupted, however, for analogs that contain cycloaliphatic groups directly substituted on the amine (**18-**
24
25 **21**) instead of being separated from the amine by a one-carbon spacer (**13, 14, 16** and **17**). Analogs
26
27 without the methylene spacer (**18-21**) are marked by a diminished KRI and binding affinity compared to
28
29 analogs with a methylene spacer, whereas the KRI values are of the same magnitude as desloratadine.
30
31 This cliff in the SKR trend was validated for a subset of analogs by studying the kinetics of functional H_1R
32
33 antagonism, which is known to reflect differential residence times at the H_1R .⁴⁶ Representative analogs
34
35 in which the cycloaliphatic group is substituted with a one-carbon spacer (**14, 16** and **17**) completely
36
37 inhibit the functional response of the H_1R for at least 2 hours after removal of unbound ligands, as was
38
39 observed for rupatadine. In contrast, analogs with the same cycloaliphatic groups without a one-carbon
40
41 spacer (**19-21**) allowed a clear recovery of the H_1R functional response, as was also observed for
42
43 desloratadine. Hence, the relevance of the methylene-spacer for the binding kinetics of analogs with
44
45 relatively large N-substituents was confirmed by the duration of functional H_1R inhibition.
46
47
48 The observed residence time/affinity cliff correlated with the binding poses of the representative pair **14**
49
50 and **19** in the H_1R binding pocket. Our docking studies suggest that the reduced flexibility of the
51
52
53
54
55
56
57
58
59
60

1
2
3 cycloaliphatic group without a spacer (**19**) might lead to a suboptimal fit due to steric hindrance (Figure
4 5C, D). The increase in ligand residence time at the H₁R, as was observed for most analogs with an
5 aliphatic group on the basic amine of desloratadine (*vide supra*), seems therefore to be mitigated when
6 the shape of the H₁R binding pocket, i.e. the steric constraints imposed by residues I454^{7,39} and Y458^{7,43},
7 is interfering with the binding position of the desloratadine scaffold.
8
9

10 Recently, it was shown that N-methylation of H₁R ligands with a primary or secondary amine increased
11 the binding affinity at the H₁R by displacing a water molecule near I454^{7,39}.⁴² However, this effect on the
12 binding affinity was not observed for analogs with a chlorine moiety on the aromatic rings. Consistent
13 with this finding, N-methylation of desloratadine (which contains a chlorine group), affording **24**, had
14 only modest effects on the H₁R binding affinity. Interestingly, **24** did have a higher KRI compared to
15 desloratadine but not to the same extent as was observed for larger aliphatic substituents (e.g. **13-17**).
16 Substitution with aliphatic or aromatic groups on the piperidine possibly reduces the resolution of both
17 the ligand and binding site during a dissociation event. For ligand dissociation from the CRF₁R, for
18 example, a low degree of ligand solvation during egress from the pocket was related to a long residence
19 time at the receptor.⁴⁰ Moreover, hydrophobic shielding of H-bonds can increase the lifetime of such
20 interactions and consequently result in an increased residence time.³⁹ This is corroborated by the fact
21 that ligands with a relatively high KRI (>1.5) were relatively lipophilic (logD_{7.4}, Supplementary Figure 1).
22 Considering that N-substitution of H₁R ligands was shown to interfere with the water network in the
23 binding site⁵⁴ and that the salt bridge between the basic amine of ligands and D107^{3,32} is crucial for a
24 high binding affinity at the receptor,⁴¹ shielding this interaction pair might prevent a rapid egress of the
25 ligands from the binding site.
26
27
28
29
30
31
32
33
34
35
36
37
38
39
40
41
42
43
44
45
46
47
48
49

50 In conclusion, compared to desloratadine, rupatadine has an extremely long residence time at the H₁R
51 despite an apparent loss in binding affinity, resulting in a longer duration of functional H₁R antagonism.
52 Development of a [³H]levocetirizine radiolabel allowed a detailed SKR study, which shows that aliphatic
53
54
55
56
57
58
59
60

1
2
3 N-substitution of the piperidine ring from desloratadine is enough to obtain antagonists with a long
4 residence time at the H₁R without increasing the observed binding affinity. Analogs with large flexible
5 residence time at the H₁R without increasing the observed binding affinity. Analogs with large flexible
6 residence time at the H₁R without increasing the observed binding affinity. Analogs with large flexible
7 cycloaliphatic or aromatic substituents, like the (5-methylpyridin-3-yl)methyl substituent of rupatadine,
8 have a long residence time at the H₁R. Notably, analogs with cycloaliphatic substituents required an
9 additional methylene spacer on the amine for an optimal binding of the H₁R. Modeling studies suggest
10 that the combined affinity/kinetics profiles of analogs without a methylene spacer are possibly linked to
11 the steric complementarity in the ligand-H₁R complex. Aliphatic N-substitution of H₁R antagonists is a
12 new potential strategy to optimize the residence time at the receptor. The presented SKR highlights that
13 subtle structural changes of small-molecule ligands can have a profound effect on the binding kinetics at
14 GPCRs.
15
16
17
18
19
20
21
22
23
24

25 **Experimental section**

26 **Pharmacological assays**

27
28 All compounds that were tested in pharmacological assays (**1-24, 28**) are confirmed to pass a publicly
29 available PAINS filter.^{55,56}
30
31
32
33

34 **Radioligand binding experiments**

35
36 Radioligand binding experiments were performed as described before, with minor alterations.²⁶ Cell
37 pellets were produced from HEK293T cells expressing the N-terminally HA-tagged H₁R, and pellets were
38 stored at -20 °C. Upon experimentation, cells were thawed, resuspended in radioligand binding buffer
39 [Na₂HPO₄ (50 mM) and KH₂PO₄ (50 mM), pH 7.4] and homogenized with a Branson sonifier 250 (Branson
40 Ultrasonics, Danbury, CT, USA). Cell homogenates (0.5 – 3 µg/well) were then incubated with the
41 respective ligands under gentle agitation, as specified for the various assay formats below. After the
42 incubation time, binding reactions were terminated with the cell harvester (Perkin Elmer) using rapid
43 filtration and wash steps over PEI-coated GF/C filter plates. Filter bound radioligand was then quantified
44 by scintillation counting using Microscint-O and the Wallac Microbeta counter (Perkin Elmer).
45
46
47
48
49
50
51
52
53
54
55
56
57
58
59
60

1
2
3 In *competition binding experiments*, cell homogenates were incubated for 4 h at 25 °C with a single
4 concentration of [³H]mepyramine (1.5 – 4nM) and increasing concentrations unlabeled ligands (10⁻⁵ M –
5 10⁻¹³ M). IC₅₀ values were obtained by analyzed the displacement curves with GraphPad Prism 7.03
6 (GraphPad Software, San Diego, USA) and were converted to K_i values using the Cheng-Prusoff
7 equation.⁵⁷

8
9
10 The binding rate constants of [³H]levocetirizine were determined using the previously described
11 methodology, by using four different concentrations of [³H]levocetirizine (1 – 35 nM) for a total
12 incubation time of 360 min, with an incubation temperature of 37 °C (data not shown).²⁶ This resulted in
13 a k_{on} of 3.7 ± 0.4 10⁶·min⁻¹·M⁻¹ and a k_{off} of 0.022 ± 0.003 min⁻¹. In *competitive association experiments*
14 with [³H]levocetirizine as radioligand, cell homogenates were incubated at 37°C for various incubation
15 times with a single concentration of [³H]levocetirizine (5 – 8 nM) in the absence of unlabeled ligand as
16 well as with three different concentrations of either desloratadine (2 – 60 nM) or rupatadine (0.1 – 7
17 nM). The k_{on} and k_{off} values for the binding of [³H]levocetirizine are constrained during the analysis of
18 the H₁R binding kinetics of desloratadine and rupatadine. Kinetic binding rate constants as well as their
19 asymmetrical 95% confidence intervals (95% CI) were determined using GraphPad Prism 7.03. Since the
20 95% CI values were very broad, values are depicted to be higher or lower than the 95% CI boundary
21 value observed over all individually performed experiments. Graphs depict a representative graph with
22 mean and SD of duplicate values showing, for clarity, only a single concentration unlabeled ligand.

23
24
25 *Competitive association experiments* with [³H]mepyramine as radioligand were performed as described
26 before, with minor alterations.²⁶ Briefly, cell homogenates were incubated at 25°C for various incubation
27 times with a single concentration of [³H]mepyramine (2.5 nM – 5.5 nM) in the absence or presence of a
28 single concentration unlabeled ligand (desloratadine [4 – 8 nM] or rupatadine [80 – 250 nM]).

29
30
31 In *dual-point competition association* experiments the kinetic rate index (KRI) value at the H₁R is
32 determined. Cell homogenates were incubated on a 96-well plate for 1 h and 6 h at 37°C, with a single
33

1
2
3 concentration of [³H]levocetirizine (4 – 11 nM) together with a single concentration of unlabeled ligand
4 that equals the respective K_i-value of that ligand at the H₁R. All conditions were measured in triplicate
5
6 per experiment (n=3). Additionally, for each 96-well plate, [³H]levocetirizine was incubated with a large
7
8 excess of mianserin (10⁻⁵ M) to determine non-specific binding levels of the radioligand (n=6) and, as a
9
10 positive control, [³H]levocetirizine binding was determined in the absence of competitor (maximal
11
12 binding, n=6). [³H]levocetirizine binding levels were baseline corrected by subtracting non-specific
13
14 binding levels and KRI values were then calculated by the ratio of [³H]levocetirizine binding after a 1 h
15
16 incubation time over the [³H]levocetirizine binding after a 6 h incubation time. KRI-values are a
17
18 quantitative measure for the overshoot in radioligand binding, which results from incubating the
19
20 radioligand with an unlabeled ligand that has a relatively low k_{off}.^{29,30} It is therefore crucial that the
21
22 concentrations of unlabeled ligands are comparable and lead to a sub-maximal inhibition of the
23
24 radioligand binding. Therefore KRI-values were only accepted when the %-inhibition of [³H]levocetirizine
25
26 binding (compared to the maximal [³H]levocetirizine binding) was (1) less than 80% after either 1 or 6 h
27
28 and (2) more than 20% inhibition after 6 h. In the case that data points had to be excluded, the
29
30 concentration unlabeled ligands were attenuated (ranging from 1 x K_i to 3 x K_i concentrations). All
31
32 experiments were performed in triplicate or more.
33
34
35
36
37
38

39 **Intracellular calcium mobilization assay**

40
41 The functional recovery of the H₁R following antagonism was measured as described before.⁴⁶ In short,
42
43 HeLa cells, endogenously expressing the H₁R, were seeded 2·10⁴ cells/well in a clear bottom 96-well
44
45 plate which were pre-incubated overnight with a concentration antagonist corresponding to 10 times
46
47 the respective K_i at the H₁R (24 wells per antagonist). After 18-20 h, cells were labeled with the Fluo-
48
49 4NW dye in the presence of the respective concentration antagonist for an hour. Both the excess dye-
50
51 solution as well as the unbound antagonists were removed by washing the cells two times and cells
52
53 were then reconstituted in HBSS buffer supplemented with probenecid (2.5 mM) (t₀). Following the
54
55
56
57
58
59
60

1
2
3 wash step, cells were stimulated every 5 min by histamine injection, into a single well, using the
4
5 NOVOstar plate reader (BMG Labtech, Ortenberg, Germany), while simultaneously detecting the calcium
6
7 mediated Fluo4NW fluorescence ($\lambda_{\text{excitation}}$ 494 nm and $\lambda_{\text{emission}}$ 516 nm). For each well stimulated with
8
9 histamine, a consecutive triton-x100 injection after 65 sec was used to lyse the cells leading to
10
11 saturation of the Fluo4 NW with calcium. The histamine-induced peak-response was then normalized to
12
13 basal levels of fluorescence (prior to histamine injection; 0) and saturated Fluo4 NW fluorescence
14
15 (following Triton X-100 injection; 1). This led to a reproducible histamine induced response over time for
16
17 HeLa cells pretreated with vehicle condition, which was set to a 100%. Histamine-induced peak-
18
19 responses were plotted against the difference in time between t_0 and the subsequent histamine
20
21 injection. The recovery time (RecT) was determined for antagonists by non-linear regression using the
22
23 one-phase association model in GraphPad Prism 7.03.
24
25
26

27 **Molecular modeling**

28
29 SMILES for compounds **1-24** were obtained from ChemBioDraw Ultra (version 16.0.1.4), and were
30
31 subsequently used as input for ChemAxon's calculator for protonation (pH = 7.4). A 3D conformation
32
33 was then generated using Molecular Networks' CORINA (version 3.49) and stored in Tripos MOL2 format
34
35 (gold extension). The doxepin-bound H₁R structure was obtained from the protein data bank (PDB-code
36
37 3RZE) after which the fused T4-lysozyme was removed from the structure. The complex was further
38
39 prepared for docking using MOE (Chemical Computing Group, version 2016.0802). Using PLANTS
40
41 (version 1.2)⁴⁸ each compound was docked into the H₁R binding pocket 3-times with the following
42
43 settings: search speed 1, cluster rmsd 1.0, cluster structures 10, and scored using the ChemPLP scoring
44
45 function. The binding site was defined by the center of the co-crystallized ligand doxepin with a radius of
46
47 11Å. The resulting docking poses were visually inspected and the poses with the best overlap with each
48
49 other as well as the doxepin reference compound were selected, which were also the highest-ranking
50
51 poses for each compound. Moreover, using an interaction fingerprint similarity analysis⁵⁸ all docking
52
53
54
55
56
57
58
59
60

1
2
3 poses were compared to the binding mode of the co-crystallized compound Doxepin. All selected
4
5 docking poses have an interaction fingerprint similarity of at least 0.72 compared to the binding mode of
6
7 Doxepin and are depicted in the supporting information (Figure S2-S3). The binding mode figures were
8
9 created with PyMol (version 1.8.0).
10

11 12 **Chemistry**

13 14 **General procedures**

15 16 17 **Synthesis of rupatadine analogs 3-24**

18
19 Anhydrous THF, DCM, DMF, and Et₂O were obtained by elution through an activated alumina column prior
20
21 to use. All other solvents and chemicals were acquired from commercial suppliers and were used as
22
23 received. ChemBioDraw Ultra 16.0.1.4 was used to generate systematic names for all molecules. All
24
25 reactions were performed under an inert atmosphere (N₂). TLC analyses were carried out with alumina
26
27 silica plates (Merck F₂₅₄) using staining and/or UV visualization. Column purifications were performed
28
29 manually using Silicycle Ultra Pure silica gel or automatically using Biotage equipment. NMR spectra (¹H,
30
31 ¹³C, and 2D) were recorded on a Bruker 300 (300 MHz), Bruker 500 (500 MHz) or a Bruker 600 (600 MHz)
32
33 spectrometer. Chemical shifts are reported in ppm (δ) and the residual solvent was used as internal
34
35 standard (δ ¹H NMR: CDCl₃ 7.26; DMSO-d₆ 2.50; CD₃OD 3.31; δ ¹³C NMR: CDCl₃ 77.16; DMSO-d₆ 39.52;
36
37 CD₃OD 49.00). Data are reported as follows: chemical shift (integration, multiplicity (s = singlet, d =
38
39 doublet, t = triplet, q = quartet, br = broad signal, m = multiplet, app = apparent), and coupling constants
40
41 (Hz)). A Bruker microTOF mass spectrometer using ESI in positive ion mode was used to record HRMS
42
43 spectra. A Shimadzu LC-20AD liquid chromatograph pump system linked to a Shimadzu SPD-M20A diode
44
45 array detector with MS detection using a Shimadzu LC-MS-2010EV mass spectrometer was used to
46
47 perform LC-MS analyses. An Xbridge (C18) 5 μm column (50 mm, 4.6 mm) was used. The solvents that
48
49 were used were the following: solvent B (acetonitrile with 0.1% formic acid) and solvent A (water with
50
51 0.1% formic acid), flow rate of 1.0 mL/min, start 5% B, linear gradient to 90% B in 4.5 min, then 1.5 min at
52
53
54
55
56
57

1
2
3 90% B, then linear gradient to 5% B in 0.5 min, then 1.5 min at 5% B; total run time of 8 min. All compounds
4
5 have a purity of $\geq 95\%$ (unless specified otherwise), calculated as the percentage peak area of the analyzed
6
7 compound by UV detection at 254 nm (values are rounded). Reverse-phase column chromatography
8
9 purifications were performed using Buchi PrepChem C-700 equipment with a discharge deuterium lamp
10
11 ranging from 200-600 nm to detect compounds using solvent B (acetonitrile with 0.1% formic acid),
12
13 solvent A (water with 0.1% formic acid), flow rate of 15.0 mL/min and a gradient (start 95% A for 3.36 min,
14
15 then linear gradient to 5% A in 30 min, then at 5% A for 3.36 min, then linear gradient to 95% A in 0.5 min,
16
17 then 1.5 min at 95% A).
18
19

20
21 The Supporting Information lists ^1H -NMR and ^{13}C -NMR spectroscopy data as well as high-resolution
22
23 mass spectroscopy and LC-MS chromatograms (Figure S4 – Figure S69).
24

25 **Synthesis of [^3H]levocetirizine (25-28)**

26
27 Column chromatography was carried out using pre-packed silica gel cartridges (SiliCycle, Quebec, Canada)
28
29 on an Isco Companion (Teledyne Isco, NE, USA). ^1H NMR spectra were recorded on a Bruker (600 MHz or
30
31 400 MHz) using the stated solvent. Chemical shifts (δ) in ppm are quoted relative to CDCl_3 (δ 7.26 ppm)
32
33 and DMSO-d_6 (δ 2.50 ppm). Liquid chromatography-mass spectrometry (LC-MS) data was collected using
34
35 a Waters Alliance LC (Waters Corporation, MA, USA) with Waters ZQ mass detector. Analytical HPLC data
36
37 was recorded using Agilent 1200 HPLC system with a β -Ram Flow Scintillation Analyser, using the following
38
39 conditions: Waters Sunfire C_{18} , 3.5 μm , 4.6 x 100 mm column at 40°C, eluting with 5% acetonitrile/water
40
41 + 0.1% TFA to 95% acetonitrile/water + 0.1% TFA over a 32 minute gradient. Specific activities were
42
43 determined gravimetrically with a Packard TriCarb 2100CA Liquid Scintillation Analyser (Packard
44
45 Instrument Company Inc., IL, USA) using Ultima GoldTM cocktail. Reactions with tritium gas were carried
46
47 out on a steel manifold obtained from RC Tritec AG (Teufen, Switzerland). Specific activity was calculated
48
49 by comparison of the ratio of tritium/hydrogen or carbon-14/carbon-12 for the tracer against the
50
51 unlabelled reference. [^3H]Methyl nosylate was obtained from Quotient Bioresearch as a solution in
52
53
54
55
56
57

1
2
3 toluene at 3150 GBq mmol⁻¹. Tritium gas was supplied absorbed onto a depleted uranium bed by RC Tritec
4
5 AG (Teufen, Switzerland). All other reagents and solvents were obtained from Sigma-Aldrich and Fisher
6
7 and were used without further purification.
8

9 10 **Detailed experimental procedures**

11 **8-chloro-11-(1-((4-methylpyridin-3-yl)methyl)piperidin-4-ylidene)-6,11-dihydro-5H-**

12 **benzo[5,6]cyclohepta[1,2-b]pyridine (3)**

13
14
15
16 A mixture of 4-methylnicotinaldehyde (93 mg, 0.77 mmol), desloratadine (200 mg, 0.643 mmol) and
17
18 NaBH(OAc)₃ (218 mg, 1.027 mmol) in DCE (10 mL) was stirred at room temperature for 12 h. The resulting
19
20 solution was diluted with water and extracted with DCM. The organic phase was washed with satd. aq.
21
22 NaHCO₃-solution. The organic layer was dried over Na₂SO₄, filtered and concentrated under vacuum. The
23
24 crude mixture was purified by reverse-phase column chromatography (H₂O/MeCN/HCOOH). The product
25
26 fraction was evaporated, extracted with DCM/satd. aq. Na₂CO₃ solution, dried (MgSO₄) and concentrated
27
28 to yield the title compound as a pink foam (170 mg, 64% yield).
29

30
31
32 ¹H NMR (500 MHz, CDCl₃) δ 8.42 – 8.22 (m, 3H), 7.39 (dd, *J* = 7.6, 1.3 Hz, 1H), 7.15 – 6.97 (m, 5H), 3.48 –
33
34 3.25 (m, 4H), 2.87 – 2.60 (m, 4H), 2.51 – 2.20 (m, 7H), 2.19 – 2.04 (m, 2H). ¹³C NMR (126 MHz, CDCl₃) δ
35
36 157.46, 150.18, 148.22, 147.40, 146.49, 139.49, 138.86, 137.76, 137.35, 133.43, 132.62, 132.56, 132.41,
37
38 130.79, 128.94, 125.98, 125.43, 122.13, 57.98, 54.80, 54.71, 31.79, 31.40, 30.97, 30.76, 18.81. HRMS:
39
40 C₂₆H₂₇ClN₃ (M+H)⁺ calcd: 416.1894, found: 416.1883. LC-MS: t_R = 3.0 min, purity >96% (254 nm), m/z: 416.2
41
42 (M+H)⁺.
43
44
45
46
47

48 **8-chloro-11-(1-((2-methylpyridin-3-yl)methyl)piperidin-4-ylidene)-6,11-dihydro-5H-**

49 **benzo[5,6]cyclohepta[1,2-b]pyridine (4)**

50
51
52 A mixture of desloratadine (155 mg, 0.50 mmol), 3-(chloromethyl)-2-methylpyridine hydrochloride (116
53
54 mg, 0.65 mmol) and K₂CO₃ (180 mg, 1.30 mmol) in DMF (10 mL) was stirred at room temperature for 18
55
56
57

1
2
3 h. The mixture was diluted with EtOAc, washed with water (2x) and brine, dried over Na₂SO₄, filtered and
4
5 concentrated under vacuum. The crude mixture was purified by reverse-phase column chromatography
6
7 (H₂O/MeCN/HCOOH) to yield the title compound as a pink foam (120 mg, 58% yield).

8
9
10 ¹H NMR (500 MHz, CDCl₃) δ 8.42 – 8.31 (m, 2H), 7.59 (d, *J* = 7.0 Hz, 1H), 7.42 (d, *J* = 7.6 Hz, 1H), 7.16 – 7.02
11
12 (m, 5H), 3.49 – 3.29 (m, 4H), 2.88 – 2.65 (m, 4H), 2.60 – 2.45 (m, 4H), 2.45 – 2.26 (m, 3H), 2.23 – 2.06 (m,
13
14 2H). ¹³C NMR (126 MHz, CDCl₃) δ 157.62, 157.44, 147.40, 146.61, 139.50, 138.78, 137.76, 137.32, 137.01,
15
16 133.37, 132.69, 132.59, 131.89, 130.78, 128.92, 125.98, 122.11, 121.00, 59.61, 54.92, 54.84, 31.77, 31.41,
17
18 30.95, 30.72, 22.26. HRMS: C₂₆H₂₇ClN₃ (M+H)⁺ calcd: 416.1888, found: 416.1906. LC-MS: t_R = 2.9 min,
19
20 purity >98% (254 nm), m/z: 416.2 (M+H)⁺.
21
22
23
24

25 **8-chloro-11-(1-((6-methylpyridin-3-yl)methyl)piperidin-4-ylidene)-6,11-dihydro-5H-**

26 **benzo[5,6]cyclohepta[1,2-b]pyridine (5)**

27
28
29
30 A mixture of desloratadine (200 mg, 0.643 mmol), 5-(bromomethyl)-2-methylpyridine hydrobromide (224
31
32 mg, 0.836 mmol) and K₂CO₃ (231 mg, 1.67 mmol) in DMF (10 mL) was stirred at room temperature for 18
33

34
35 h. The mixture was diluted with EtOAc, washed with water (2x) and brine, dried over Na₂SO₄, filtered and
36
37 concentrated under vacuum. The crude mixture was purified by reverse-phase column chromatography
38
39 (H₂O/MeCN/HCOOH). The product fraction was evaporated, extracted with DCM/satd. aq. Na₂CO₃
40
41 solution, dried (MgSO₄) and concentrated to yield the title compound as a pink foam (170 mg, 64% yield).

42
43 ¹H NMR (500 MHz, CDCl₃) δ 8.41 – 8.33 (m, 2H), 7.60 (d, *J* = 7.3 Hz, 1H), 7.41 (d, *J* = 7.6 Hz, 1H), 7.16 – 7.02
44
45 (m, 5H), 3.50 (s, 2H), 3.42 – 3.28 (m, 2H), 2.86 – 2.68 (m, 4H), 2.57 – 2.48 (m, 4H), 2.47 – 2.12 (m, 5H). ¹³C
46
47 NMR (126 MHz, CDCl₃) δ 157.41, 157.37, 149.71, 146.60, 139.51, 138.20, 137.70, 137.42, 137.32, 133.38,
48
49 133.00, 132.69, 130.70, 130.1, 128.95, 126.01, 123.01, 122.14, 59.62, 54.56, 54.45, 31.76, 31.42, 30.64,
50
51 30.39, 24.10. HRMS: C₂₆H₂₇ClN₃ (M+H)⁺ calcd: 416.1894, found: 416.1886. LC-MS: t_R = 3.0 min, purity >98%
52
53 (254 nm), m/z: 416.2 (M+H)⁺.
54
55
56
57

1
2
3
4
5 **8-chloro-11-(1-(pyridin-3-ylmethyl)piperidin-4-ylidene)-6,11-dihydro-5H-benzo[5,6]cyclohepta[1,2-**
6
7
8 **b]pyridine (6)**

9
10 A mixture of desloratadine (500mg, 1.61mmol), 3-(bromomethyl)-pyridine hydrobromide (529 mg, 2.09
11 mmol) and K₂CO₃ (579 mg, 4.19 mmol) in DMF (10 mL) was stirred at room temperature for 18 h. The
12 mixture was diluted with EtOAc, washed with water (2x) and brine, dried over Na₂SO₄, filtered and
13 concentrated under vacuum. The crude mixture was purified by reverse-phase column chromatography
14 (H₂O/MeCN/HCOOH) to yield the title compound as a pink foam (430 mg, 66% yield).
15
16

17
18
19 ¹H NMR (500 MHz, CDCl₃) δ 8.54 – 8.43 (m, 2H), 8.37 (d, *J* = 4.6 Hz, 1H), 7.67 (d, *J* = 7.7 Hz, 1H), 7.41 (d, *J*
20 = 7.6 Hz, 1H), 7.25 – 7.20 (m, 1H), 7.15 – 7.02 (m, 4H), 3.49 (s, 2H), 3.43 – 3.27 (m, 2H), 2.88 – 2.64 (m,
21 4H), 2.55 – 2.46 (m, 1H), 2.45 – 2.25 (m, 3H), 2.21 – 2.02 (m, 2H). ¹³C NMR (126 MHz, CDCl₃) δ 157.44,
22 150.40, 148.60, 146.63, 139.51, 138.60, 137.73, 137.34, 136.81, 133.63, 133.40, 132.79, 132.63, 130.81,
23 128.96, 126.01, 123.37, 122.15, 60.04, 54.73, 54.66, 31.80, 31.42, 30.89, 30.65. HRMS: C₂₅H₂₅ClN₃ (M+H)⁺
24
25 calcd: 402.1737, found: 402.1733. LC-MS: t_R = 3.0 min, purity >99% (254 nm), m/z: 402.1 (M+H)⁺.
26
27
28
29
30
31
32
33
34
35

36
37 **8-chloro-11-(1-(pyridin-4-ylmethyl)piperidin-4-ylidene)-6,11-dihydro-5H-benzo[5,6]cyclohepta[1,2-**
38
39 **b]pyridine (7)**

40
41 A mixture of desloratadine (500 mg, 1.61 mmol), 4-(bromomethyl)-pyridine hydrobromide (529 mg, 2.09
42 mmol) and K₂CO₃ (579 mg, 4.19 mmol) in DMF (10 mL) was stirred at room temperature for 18 h. The
43 mixture was diluted with EtOAc, washed with water (2x) and brine, dried over Na₂SO₄, filtered and
44 concentrated under vacuum. The crude mixture was purified by reverse-phase column chromatography
45 (H₂O/MeCN/HCOOH) to yield the title compound as a pink foam (229 mg, 36% yield).
46
47

48
49
50 ¹H NMR (500 MHz, CDCl₃) δ 8.49 (d, *J* = 5.6 Hz, 2H), 8.35 (d, *J* = 4.6 Hz, 1H), 7.39 (d, *J* = 7.6 Hz, 1H), 7.24 (d,
51
52
53
54
55
56
57
58
59
60
J = 5.4 Hz, 2H), 7.16 – 7.00 (m, 4H), 3.46 (s, 2H), 3.42 – 3.24 (m, 2H), 2.85 – 2.60 (m, 4H), 2.57 – 2.23 (m,

1
2
3 4H), 2.20 – 2.04 (m, 2H). ¹³C NMR (126 MHz, CDCl₃) δ 157.38, 149.64, 147.76, 146.58, 139.50, 138.46,
4
5 137.69, 137.38, 133.41, 132.82, 132.63, 130.78, 128.96, 126.00, 123.89, 122.18, 61.56, 54.85, 54.82,
6
7 31.77, 31.40, 30.89, 30.67. HRMS: C₂₅H₂₅ClN₃ (M+H)⁺ calcd: 402.1737, found: 402.1741. LC-MS: t_R = 3.0
8
9 min, purity >99% (254 nm), m/z: 402.1 (M+H)⁺.

11
12
13
14 **8-chloro-11-(1-(pyridin-2-ylmethyl)piperidin-4-ylidene)-6,11-dihydro-5H-benzo[5,6]cyclohepta[1,2-**
15
16 **b]pyridine (8)**

17
18 A mixture of desloratadine (500 mg, 1.61 mmol), 2-(bromomethyl)-pyridine hydrobromide (529 mg, 2.09
19
20 mmol) and K₂CO₃ (579 mg, 4.19 mmol) in DMF (10 mL) was stirred at room temperature for 18 h. The
21
22 mixture was diluted with EtOAc, washed with water (2x) and brine, dried over Na₂SO₄, filtered and
23
24 concentrated under vacuum. The crude mixture was purified by reverse-phase column chromatography
25
26 (H₂O/MeCN/HCOOH) to yield the title compound as a pink foam (399 mg, 62% yield).

27
28 ¹H NMR (500 MHz, CDCl₃) δ 8.52 (d, *J* = 4.5 Hz, 1H), 8.36 (d, *J* = 4.6 Hz, 1H), 7.62 (t, *J* = 7.6 Hz, 1H), 7.40 (d,
29
30 *J* = 7.2 Hz, 2H), 7.18 – 6.98 (m, 5H), 3.63 (s, 2H), 3.45 – 3.27 (m, 2H), 2.87 – 2.68 (m, 4H), 2.59 – 2.40 (m,
31
32 2H), 2.40 – 2.27 (m, 2H), 2.26 – 2.10 (m, 2H). ¹³C NMR (126 MHz, CDCl₃) δ 158.54, 157.56, 149.24, 146.60,
33
34 139.52, 138.86, 137.75, 137.28, 136.44, 133.43, 132.62, 132.57, 130.87, 128.96, 125.97, 123.22, 122.11,
35
36 122.06, 64.46, 55.07, 55.05, 31.82, 31.40, 30.94, 30.71. HRMS: C₂₅H₂₅ClN₃ (M+H)⁺ calcd: 402.1737, found:
37
38 402.1738. LC-MS: t_R = 3.1 min, purity >99% (254 nm), m/z: 402.1 (M+H)⁺.

39
40
41
42
43
44
45 **8-chloro-11-(1-(pyrimidin-2-ylmethyl)piperidin-4-ylidene)-6,11-dihydro-5H-benzo[5,6]cyclohepta[1,2-**
46
47 **b]pyridine (9)**

48
49 A mixture of pyrimidine-2-carbaldehyde (91 mg, 0.84 mmol), desloratadine (218 mg, 0.7 mmol) and
50
51 NaBH(OAc)₃ (237 mg, 1.12 mmol) in DCE (10 mL) was stirred at room temperature for 12 h. The resulting
52
53 solution was diluted with water and extracted with DCM. The organic phase was washed with satd. aq.
54
55
56
57

1
2
3 NaHCO₃. The organic layer was dried over Na₂SO₄, filtered and concentrated under vacuum. The crude
4
5 mixture was purified by column chromatography (EtOAc/MeOH/TEA = 94:4:2, v/v/v) to yield the title
6
7 compound as a pink foam (240 mg, 85% yield).

8
9
10 ¹H NMR (500 MHz, CDCl₃) δ 8.71 (d, *J* = 4.9 Hz, 2H), 8.37 (dd, *J* = 4.7, 1.4 Hz, 1H), 7.41 (dd, *J* = 7.7, 1.4 Hz,
11
12 1H), 7.17 (t, *J* = 4.9 Hz, 1H), 7.14 – 7.02 (m, 4H), 3.86 – 3.74 (m, 2H), 3.44 – 3.30 (m, 2H), 2.89 – 2.71 (m,
13
14 4H), 2.65 – 2.47 (m, 2H), 2.42 – 2.25 (m, 4H). ¹³C NMR (126 MHz, CDCl₃) δ 167.63, 157.64, 157.20, 146.59,
15
16 139.48, 138.78, 137.73, 137.20, 133.43, 132.61, 132.59, 130.89, 128.96, 125.97, 122.07, 119.32, 65.09,
17
18 55.25, 55.21, 31.85, 31.40, 30.75, 30.50.

19
20
21 HRMS: C₂₄H₂₄ClN₄ (M+H)⁺ calcd: 403.1684, found: 403.1680. LC-MS: t_R = 2.9 min, >99% (254 nm), m/z:
22
23 403.2 (M+H)⁺.

24
25
26
27
28 **8-chloro-11-(1-(pyrimidin-4-ylmethyl)piperidin-4-ylidene)-6,11-dihydro-5H-benzo[5,6]cyclohepta[1,2-**
29
30 **b]pyridine (10)**

31
32 A mixture of pyrimidine-4-carbaldehyde (91 mg, 0.84 mmol), desloratadine (218 mg, 0.7 mmol) and
33
34 NaBH(OAc)₃ (237 mg, 1.12 mmol) in DCE (10 mL) was stirred at room temperature for 12 h. The resulting
35
36 solution was diluted with water and extracted with DCM. The organic phase was washed with satd. aq.
37
38 NaHCO₃, dried over Na₂SO₄, filtered and concentrated under vacuum. The crude mixture was purified by
39
40 column chromatography (EtOAc/MeOH/TEA = 94:4:2, v/v/v) to yield the title compound as a pink foam
41
42 (248 mg, 88% yield).

43
44
45 ¹H NMR (500 MHz, CDCl₃) δ 9.11 (s, 1H), 8.67 (d, *J* = 5.2 Hz, 1H), 8.38 (dd, *J* = 4.7, 1.2 Hz, 1H), 7.53 (d, *J* =
46
47 5.0 Hz, 1H), 7.42 (dd, *J* = 8.8, 1.2 Hz, 2H), 7.17 – 7.02 (m, 4H), 3.62 (s, 2H), 3.44 – 3.31 (m, 2H), 2.87 – 2.71
48
49 (m, 4H), 2.61 – 2.52 (m, 1H), 2.51 – 2.42 (m, 1H), 2.41 – 2.31 (m, 2H), 2.30 – 2.19 (m, 2H). ¹³C NMR (126
50
51 MHz, CDCl₃) δ 167.86, 158.57, 157.38, 157.09, 146.59, 139.52, 138.13, 137.71, 137.37, 133.42, 133.05,
52
53 132.71, 130.74, 128.96, 126.03, 122.17, 120.13, 63.36, 55.10, 31.79, 31.44, 30.92, 30.70, one signal
54
55

1
2
3 overlapping or not visible. HRMS: C₂₄H₂₄ClN₄ (M+H)⁺ calcd: 403.1684, found: 403.1681. LC-MS: t_R = 2.9
4
5 min, 99% (254 nm), m/z: 403.2 (M+H)⁺.
6
7
8
9

10 **8-chloro-11-(1-(3-methylbenzyl)piperidin-4-ylidene)-6,11-dihydro-5H-benzo[5,6]cyclohepta[1,2-**
11 **b]pyridine (11)**

12
13
14 Desloratadine (500 mg, 1.61 mmol) was added to 3-methylbenzyl bromide (387 mg, 2.09 mmol) and TEA
15
16 (326 mg, 3.22 mmol) in DCM (10 mL). The resulting mixture was stirred at room temperature for 18 h. The
17
18 solution was then diluted with DCM, washed with a 5% NaHCO₃ solution, then with H₂O, dried over
19
20 Na₂SO₄, filtered and concentrated under vacuum. The crude mixture was purified by reverse-phase
21
22 column chromatography (H₂O/MeCN/HCOOH). The product fraction was evaporated, extracted with
23
24 DCM/satd. aq. Na₂CO₃ solution, dried (MgSO₄) and concentrated to yield the title compound as a pink
25
26 foam (432 mg, 65% yield).
27
28

29
30 ¹H NMR (500 MHz, CDCl₃) δ 8.39 (dd, *J* = 4.8, 1.5 Hz, 1H), 7.41 (d, *J* = 7.7 Hz, 1H), 7.22 – 6.99 (m, 8H), 3.53
31
32 – 3.28 (m, 4H), 2.90 – 2.68 (m, 4H), 2.58 – 2.25 (m, 7H), 2.21 – 2.04 (m, 2H). ¹³C NMR (126 MHz, CDCl₃) δ
33
34 157.69, 146.64, 139.52, 139.18, 138.09, 137.84, 137.78, 137.23, 133.42, 132.57, 132.49, 130.92, 129.97,
35
36 128.97, 128.06, 127.79, 126.33, 125.99, 122.08, 62.99, 54.89, 54.85, 31.87, 31.44, 30.99, 30.75, 21.46.
37
38 HRMS: C₂₇H₂₈ClN₂ (M+H)⁺ calcd: 415.1941, found: 415.1938. LC-MS: t_R = 3.6 min, purity >99% (254 nm),
39
40 m/z: 415.2 (M+H)⁺.
41
42
43
44
45

46 **11-(1-benzylpiperidin-4-ylidene)-8-chloro-6,11-dihydro-5H-benzo[5,6]cyclohepta[1,2-b]pyridine (12)**

47
48 Desloratadine (500 mg, 1.61 mmol) was added to benzyl bromide (358 mg, 2.09 mmol) and TEA (326 mg,
49
50 3.22 mmol) in DCM (10 mL). The resulting mixture was stirred at room temperature for 18 h. The solution
51
52 was then diluted with DCM and H₂O and extraction was performed. The organic layer was dried over
53
54 Na₂SO₄, filtered. The crude mixture was purified by reverse-phase column chromatography
55
56
57
58
59
60

(H₂O/MeCN/HCOOH). The product fraction was evaporated, extracted with DCM/satd. aq. Na₂CO₃ solution, dried (MgSO₄) and concentrated to yield the title compound as a pink foam (484 mg, 75% yield). ¹H NMR (500 MHz, CDCl₃) δ 8.38 (dd, *J* = 4.8, 1.2 Hz, 1H), 7.42 (dd, *J* = 7.3, 1.1 Hz, 1H), 7.33 – 7.20 (m, 5H), 7.17 – 7.00 (m, 4H), 3.51 (s, 2H), 3.45 – 3.28 (m, 2H), 2.87 – 2.69 (m, 4H), 2.58 – 2.26 (m, 4H), 2.23 – 2.07 (m, 2H). ¹³C NMR (126 MHz, CDCl₃) δ 157.64, 146.62, 139.51, 139.04, 138.09, 137.81, 137.26, 133.42, 132.58, 132.54, 130.89, 129.23, 128.96, 128.21, 127.06, 125.99, 122.10, 62.91, 54.79, 54.74, 31.85, 31.42, 30.94, 30.71. HRMS: C₂₆H₂₆ClN₂ (M+H)⁺ calcd: 401.1785, found: 401.1779. LC-MS: t_R = 3.4 min, purity >99% (254 nm), m/z: 401.1 (M+H)⁺.

8-chloro-11-(1-(cyclohexylmethyl)piperidin-4-ylidene)-6,11-dihydro-5H-benzo[5,6]cyclohepta[1,2-b]pyridine (13)

A mixture of cyclohexanecarbaldehyde (95 mg, 0.84 mmol), desloratadine (218 mg, 0.70 mmol) and NaBH(OAc)₃ (238 mg, 1.12 mmol) in DCE (10 mL) was stirred at room temperature for 12 h. The resulting solution was diluted with water and extracted with DCM. The organic phase was washed with satd. aq. NaHCO₃ solution. The organic layer was dried over Na₂SO₄, filtered and concentrated under vacuum. The crude mixture was purified by column chromatography (cyclohexane/EtOAc/TEA = 40/58/2, v/v/v) to yield the title compound as a pink foam (180 mg, 63% yield).

¹H NMR (500 MHz, CDCl₃) δ 8.39 (d, *J* = 4.6 Hz, 1H), 7.42 (d, *J* = 7.6 Hz, 1H), 7.16 – 7.09 (m, 3H), 7.07 (dd, *J* = 7.7, 4.8 Hz, 1H), 3.46 – 3.29 (m, 2H), 2.86 – 2.74 (m, 2H), 2.74 – 2.63 (m, 2H), 2.55 – 2.46 (m, 1H), 2.44 – 2.25 (m, 3H), 2.14 – 1.97 (m, 4H), 1.80 – 1.60 (m, 5H), 1.50 – 1.38 (m, 1H), 1.26 – 1.07 (m, 3H), 0.91 – 0.78 (m, 2H). ¹³C NMR (126 MHz, CDCl₃) δ 157.77, 146.74, 139.66, 137.96, 137.35, 133.54, 132.70, 132.55, 130.96, 129.07, 126.10, 122.18, 65.45, 55.51, 55.41, 35.32, 32.16, 32.13, 31.94, 31.55, 30.87, 30.62, 26.82, 26.25, one aromatic signal overlapping or not visible. HRMS: C₂₆H₃₂ClN₂ (M+H)⁺ calcd: 407.2249, found: 407.2231. LC-MS: t_R = 3.6 min, purity >99% (254 nm), m/z: 407.2 (M+H)⁺.

1
2
3
4
5
6 **8-chloro-11-(1-(cyclopentylmethyl)piperidin-4-ylidene)-6,11-dihydro-5H-benzo[5,6]cyclohepta[1,2-**
7 **b]pyridine (14)**
8

9
10 A mixture of cyclopentanecarbaldehyde (83 mg, 0.84 mmol), desloratadine (218 mg, 0.70 mmol) and
11 NaBH(OAc)₃ (238 mg, 1.12 mmol) in DCE (10 mL) was stirred at room temperature for 12 h. The resulting
12 solution was diluted with water and extracted with DCM. The organic phase was washed with satd. aq.
13 NaHCO₃ solution. The organic layer was dried over Na₂SO₄, filtered and concentrated under vacuum. The
14 crude mixture was purified by column chromatography (cyclohexane/EtOAc/TEA = 40/58/2, v/v/v) to yield
15 the title compound as a pink foam (162 mg, 59% yield).
16

17
18 ¹H NMR (500 MHz, CDCl₃) δ 8.39 (d, *J* = 4.6 Hz, 1H), 7.41 (d, *J* = 7.7 Hz, 1H), 7.15 – 7.08 (m, 3H), 7.06 (dd, *J*
19 = 7.6, 4.9 Hz, 1H), 3.45 – 3.29 (m, 2H), 2.86 – 2.69 (m, 4H), 2.55 – 2.45 (m, 1H), 2.44 – 2.27 (m, 3H), 2.25
20 (d, *J* = 7.2 Hz, 2H), 2.16 – 1.96 (m, 3H), 1.77 – 1.67 (m, 2H), 1.61 – 1.43 (m, 4H), 1.22-1.12 (m, 2H). ¹³C NMR
21 (126 MHz, CDCl₃) δ 157.87, 146.72, 139.60, 137.98, 137.26, 133.50, 132.63, 132.30, 131.03, 129.03,
22 126.06, 122.11, 64.50, 55.36, 55.30, 37.60, 31.96, 31.77, 31.52, 31.09, 30.85, 25.30, one aromatic signal
23 overlapping or not visible. HRMS: C₂₅H₃₀ClN₂ (M+H)⁺ calcd: 393.2092, found: 393.2091. LC-MS: t_R = 3.2
24 min, purity >98% (254 nm), m/z: 393.2 (M+H)⁺.
25
26
27
28
29
30
31
32
33
34
35
36
37
38
39
40

41 **8-chloro-11-(1-(2-ethylbutyl)piperidin-4-ylidene)-6,11-dihydro-5H-benzo[5,6]cyclohepta[1,2-**
42 **b]pyridine (15)**
43

44
45 A mixture of 2-ethylbutanal (85 mg, 0.84 mmol), desloratadine (218 mg, 0.70 mmol) and NaBH(OAc)₃ (238
46 mg, 1.12 mmol) in DCE (10 mL) was stirred at room temperature for 12 h. The resulting solution was
47 diluted with water and extracted with DCM. The organic phase was washed with satd. aq. NaHCO₃
48 solution. The organic layer was dried over Na₂SO₄, filtered and concentrated under vacuum. The crude
49
50
51
52
53
54
55
56
57
58
59
60

1
2
3 mixture was purified by column chromatography (cyclohexane/EtOAc/TEA = 40/58/2, v/v/v) to yield the
4
5 title compound as a pink foam (186 mg, 67% yield).

6
7 ^1H NMR (500 MHz, CDCl_3) δ 8.39 (dd, $J = 4.9, 1.7$ Hz, 1H), 7.42 (dd, $J = 7.7, 1.6$ Hz, 1H), 7.16 – 7.11 (m, 3H),
8
9 7.08 (dd, $J = 7.7, 4.8$ Hz, 1H), 3.46 – 3.29 (m, 2H), 2.88 – 2.69 (m, 4H), 2.61 – 2.03 (br m, 8H), 1.49 – 1.24
10
11 (m, 5H), 0.84 (t, $J = 7.4$ Hz, 6H). ^{13}C NMR (126 MHz, CDCl_3) δ 157.95, 146.74, 139.83, 139.63, 138.06,
12
13 137.25, 133.51, 132.64, 132.27, 131.04, 129.04, 126.06, 122.10, 62.44, 55.60, 55.52, 38.06, 31.99, 31.56,
14
15 31.15, 30.92, 24.33, 10.99. HRMS: $\text{C}_{25}\text{H}_{32}\text{ClN}_2$ (M+H) $^+$ calcd: 395.2249, found: 395.2244. LC-MS: $t_{\text{R}} = 3.3$
16
17 min, purity >98% (254 nm), m/z: 395.2 (M+H) $^+$.
18
19
20
21
22

23 **8-chloro-11-(1-(cyclobutylmethyl)piperidin-4-ylidene)-6,11-dihydro-5H-benzo[5,6]cyclohepta[1,2-**
24
25 **b]pyridine (16)**

26
27 A mixture of (bromomethyl)cyclobutane (208 mg, 1.40 mmol), desloratadine (218 mg, 0.70 mmol) and
28
29 60% NaH dispersion (41.6 mg, 1.05 mmol) in DMF (10 ml) was stirred at room temperature for 10 h. The
30
31 resulting solution was diluted with water and extracted with DCM. The organic phase was washed with
32
33 satd. aq. NaHCO_3 solution. The organic layer was dried over Na_2SO_4 , filtered and concentrated under
34
35 vacuum. The crude mixture was purified by column chromatography (cyclohexane/EtOAc/TEA = 40/58/2,
36
37 v/v/v) to yield the title compound as a pink foam (150 mg, 56% yield).
38
39

40
41 ^1H NMR (500 MHz, CDCl_3) δ 8.38 (d, $J = 4.9, 1.4$ Hz, 1H), 7.41 (d, $J = 7.6$ Hz, 1H), 7.15 – 7.08 (m, 3H), 7.06
42
43 (dd, $J = 7.7, 4.8$ Hz, 1H), 3.44 – 3.30 (m, 2H), 2.85 – 2.73 (m, 2H), 2.74 - 2.66 (m, 2H), 2.56 – 2.44 (m, 2H),
44
45 2.43 – 2.25 (m, 5H), 2.12 – 1.96 (m, 4H), 1.92 – 1.80 (m, 1H), 1.79 – 1.70 (m, 1H), 1.69 – 1.58 (m, 2H). ^{13}C
46
47 NMR (126 MHz, CDCl_3) δ 157.78, 146.73, 139.60, 139.24, 137.93, 137.29, 133.49, 132.66, 132.46, 130.99,
48
49 129.03, 126.07, 122.13, 65.28, 55.13, 55.07, 34.36, 31.94, 31.53, 31.05, 30.80, 28.32, 18.93. HRMS:
50
51 $\text{C}_{24}\text{H}_{28}\text{ClN}_2$ (M+H) $^+$ calcd: 379.1936, found: 379.1923. LC-MS: $t_{\text{R}} = 3.1$ min, purity >96% (254 nm), m/z: 379.2
52
53 (M+H) $^+$.
54
55
56
57
58
59
60

1
2
3
4
5
6 **8-chloro-11-(1-(cyclopropylmethyl)piperidin-4-ylidene)-6,11-dihydro-5H-benzo[5,6]cyclohepta[1,2-**
7 **b]pyridine (17)**
8

9
10 A mixture of cyclopropanecarboxaldehyde (59 mg, 0.84 mmol), desloratadine (218 mg, 0.70 mmol) and
11 NaBH(OAc)₃ (238 mg, 1.12 mmol) in DCE (10 mL) was stirred at room temperature for 12 h. The resulting
12 solution was diluted with water and extracted with DCM. The organic phase was washed with satd. aq.
13 NaHCO₃ solution. The organic layer was dried over Na₂SO₄, filtered and concentrated under vacuum. The
14 crude mixture was purified by column chromatography (cyclohexane/EtOAc/TEA = 40/58/2, v/v/v) to yield
15 the title compound as a pink foam (132 mg, 52% yield).
16

17
18 ¹H NMR (500 MHz, CDCl₃) δ 8.39 (dd, *J* = 4.8, 1.6 Hz, 1H), 7.42 (dd, *J* = 7.7, 1.6 Hz, 1H), 7.16 – 7.09 (m, 3H),
19 7.07 (dd, *J* = 7.6, 4.7 Hz, 1H), 3.44 – 3.30 (m, 2H), 2.93 – 2.73 (m, 4H), 2.59 – 2.50 (m, 1H), 2.48 – 2.31 (m,
20 3H), 2.24 (d, *J* = 6.5 Hz, 2H), 2.21 - 2.12 (m, 2H), 0.92 – 0.79 (m, 1H), 0.53 – 0.43 (m, 2H), 0.06 (app q, 2H).
21

22
23 ¹³C NMR (126 MHz, CDCl₃) δ 157.78, 146.76, 139.61, 139.24, 137.94, 137.32, 133.51, 132.70, 132.58,
24 131.01, 129.05, 126.10, 122.17, 63.74, 55.10, 55.05, 31.96, 31.55, 31.05, 30.80, 8.52, 4.11, 4.09. HRMS:
25 C₂₃H₂₆ClN₂ (M+H)⁺ calcd: 365.1779, found: 365.1773. LC-MS: t_R = 2.9 min, purity >99% (254 nm), m/z: 365.1
26 (M+H)⁺.
27
28
29
30
31
32
33
34
35
36
37
38
39
40

41 **8-chloro-11-(1-cyclohexylpiperidin-4-ylidene)-6,11-dihydro-5H-benzo[5,6]cyclohepta[1,2-b]pyridine**
42 **(18)**
43

44
45 A mixture of cyclohexanone (82 mg, 0.84 mmol), desloratadine (218 mg, 0.70 mmol) and NaBH(OAc)₃ (238
46 mg, 1.12 mmol) in DCE (10 mL) was stirred at room temperature for 12 h. The resulting solution was
47 diluted with water and extracted with DCM. The organic phase was washed with satd. aq. NaHCO₃
48 solution. The organic layer was dried over Na₂SO₄, filtered and concentrated under vacuum. The crude
49
50
51
52
53
54
55
56
57
58
59
60

1
2
3 mixture was purified by column chromatography (cyclohexane/EtOAc/TEA = 40/58/2, v/v/v) to yield the
4
5 title compound as a pink foam (192 mg, 70% yield).

6
7 ^1H NMR (500 MHz, CDCl_3) δ 8.39 (dd, $J = 4.8, 1.5$ Hz, 1H), 7.42 (d, $J = 7.6$, 1H), 7.16 – 7.09 (m, 3H), 7.06 (dd,
8
9 $J = 7.7, 4.8$ Hz, 1H), 3.44 – 3.30 (m, 2H), 2.86 – 2.71 (m, 4H), 2.53 – 2.44 (m, 1H), 2.44 – 2.23 (m, 6H), 1.88
10
11 – 1.69 (m, 4H), 1.60 (app d, $J = 13.6$ Hz, 1H), 1.27 – 1.12 (m, 4H), 1.12 – 1.00 (m, 1H). ^{13}C NMR (126 MHz,
12
13 CDCl_3) δ 157.92, 146.74, 139.86, 139.60, 137.96, 137.25, 133.52, 132.64, 132.24, 131.10, 129.05, 126.06,
14
15 122.12, 63.76, 50.71, 50.59, 32.00, 31.64, 31.54, 31.38, 29.05, 28.91, 26.47, 26.17. HRMS: $\text{C}_{25}\text{H}_{30}\text{ClN}_2$
16
17 (M+H) $^+$ calcd: 393.2092, found: 393.2083. LC-MS: $t_{\text{R}} = 3.1$ min, purity >99% (254 nm), m/z: 393.2 (M+H) $^+$.
18
19
20
21
22

23 **8-chloro-11-(1-cyclopentylpiperidin-4-ylidene)-6,11-dihydro-5H-benzo[5,6]cyclohepta[1,2-b]pyridine**
24
25 **(19)**

26
27 A mixture of cyclopentanone (70 mg, 0.84 mmol), desloratadine (218 mg, 0.70 mmol) and $\text{NaBH}(\text{OAc})_3$
28
29 (238 mg, 1.12 mmol) in DCE (10 mL) was stirred at room temperature for 12 h. The resulting solution was
30
31 diluted with water and extracted with DCM. The organic phase was washed with satd. aq. NaHCO_3
32
33 solution. The organic layer was dried over Na_2SO_4 , filtered and concentrated under vacuum. The crude
34
35 mixture was purified by column chromatography (cyclohexane/EtOAc/TEA = 40/58/2, v/v/v) to yield the
36
37 title compound as a pink foam (189 mg, 71% yield).
38
39

40
41 ^1H NMR (500 MHz, CDCl_3) δ 8.38 (d, $J = 4.8$, 1H), 7.41 (d, $J = 7.6$ Hz, 1H), 7.15 – 7.08 (m, 3H), 7.06 (dd, $J =$
42
43 7.7, 4.8 Hz, 1H), 3.44 – 3.29 (m, 2H), 2.87 – 2.72 (m, 4H), 2.57 – 2.39 (m, 3H), 2.38 – 2.29 (m, 2H), 2.19 –
44
45 2.07 (m, 2H), 1.87 – 1.74 (m, 2H), 1.70 – 1.59 (m, 2H), 1.55 – 1.45 (m, 2H), 1.45 – 1.33 (m, 2H). ^{13}C NMR
46
47 (126 MHz, CDCl_3) δ 157.81, 146.73, 139.59, 139.45, 137.87, 137.26, 133.52, 132.66, 132.27, 131.05,
48
49 129.04, 126.07, 122.13, 67.41, 54.13, 54.10, 31.98, 31.53, 31.13, 30.85, 30.70, 24.34. HRMS: $\text{C}_{24}\text{H}_{28}\text{ClN}_2$
50
51 (M+H) $^+$ calcd: 379.1936, found: 379.1921. LC-MS: $t_{\text{R}} = 3.0$ min, purity >99% (254 nm), m/z: 379.1 (M+H) $^+$.
52
53
54
55
56
57
58
59
60

8-chloro-11-(1-cyclobutylpiperidin-4-ylidene)-6,11-dihydro-5H-benzo[5,6]cyclohepta[1,2-b]pyridine**(20)**

A mixture of cyclobutanone (59 mg, 0.84 mmol), desloratadine (218 mg, 0.70 mmol) and NaBH(OAc)₃ (238 mg, 1.12 mmol) in DCE (10 mL) was stirred at room temperature for 12 h. The resulting solution was diluted with water and extracted with DCM. The organic phase was washed with satd. aq. NaHCO₃ solution. The organic layer was dried over Na₂SO₄, filtered and concentrated under vacuum. The crude mixture was purified by column chromatography (cyclohexane/EtOAc/TEA = 40/58/2, v/v/v) to yield the title compound as a pink foam (145 mg, 57% yield).

¹H NMR (500 MHz, CDCl₃) δ 8.39 (d, *J* = 4.6 Hz, 1H), 7.42 (d, *J* = 7.6 Hz, 1H), 7.15 – 7.09 (m, 3H), 7.09 – 7.05 (m, 1H), 3.45 – 3.30 (m, 2H), 2.87 – 2.74 (m, 2H), 2.74 – 2.60 (m, 3H), 2.55 – 2.46 (m, 1H), 2.46 – 2.28 (m, 3H), 2.05 – 1.86 (m, 6H), 1.74 – 1.57 (m, 2H). ¹³C NMR (126 MHz, CDCl₃) δ 157.78, 146.77, 139.60, 139.01, 137.89, 137.33, 133.53, 132.78, 132.74, 130.99, 129.09, 126.12, 122.21, 60.32, 51.24, 51.23, 31.97, 31.53, 30.65, 30.38, 27.42, 14.35. HRMS: C₂₃H₂₆ClN₂ (M+H)⁺ calcd: 365.1779, found: 365.1772. LC-MS: t_R = 2.9 min, purity >99% (254 nm), m/z: 365.2 (M+H)⁺.

8-chloro-11-(1-cyclopropylpiperidin-4-ylidene)-6,11-dihydro-5H-benzo[5,6]cyclohepta[1,2-b]pyridine**(21)**

A mixture of (1-ethoxycyclopropoxy)trimethylsilane (347 mg, 2.00 mmol), desloratadine (622 mg, 2.00 mmol), AcOH (111 mg, 2.00 mmol) and sodium triacetoxyborohydride (604 mg, 3.20 mmol) in DCM (10 mL) was stirred at room temperature for 48 h. The resulting solution was diluted with water and extracted with DCM. The organic phase was washed with satd. aq. NaHCO₃ solution. The organic layer was dried over Na₂SO₄, filtered and concentrated under vacuum. The crude mixture was purified by reverse-phase column chromatography (H₂O/MeCN/HCOOH). The product fraction was evaporated, extracted with

1
2
3 DCM/satd. aq. Na₂CO₃ solution, dried (MgSO₄) and concentrated to yield the title compound as a pink
4
5 foam (124 mg, 17 % yield).

6
7 ¹H NMR (500 MHz, CDCl₃) δ 8.39 (dd, *J* = 4.9, 1.5 Hz, 1H), 7.43 (dd, *J* = 7.8, 1.6 Hz, 1H), 7.16 – 7.10 (m, 3H),
8
9 7.08 (dd, *J* = 7.7, 4.7 Hz, 1H), 3.45 – 3.32 (m, 2H), 2.92 – 2.74 (m, 4H), 2.50 – 2.42 (m, 1H), 2.40 – 2.26 (m,
10
11 5H), 1.60 – 1.50 (m, 1H), 0.47 – 0.35 (m, 4H). ¹³C NMR (126 MHz, CDCl₃) δ 157.85, 146.75, 139.58, 139.35,
12
13 137.95, 137.30, 133.51, 132.69, 132.66, 131.01, 129.08, 126.10, 122.17, 55.16, 38.39, 31.97, 31.52, 31.00,
14
15 30.74, 6.09, one aliphatic signal overlapping or not visible. HRMS: C₂₂H₂₄ClN₂ (M+H)⁺ calcd: 351.1623 ,
16
17 found: 351.1610. LC-MS: t_R = 2.9 min, purity >98% (254 nm), m/z: 351.2 (M+H)⁺.
18
19
20
21
22

23 **8-chloro-11-(1-isopropylpiperidin-4-ylidene)-6,11-dihydro-5H-benzo[5,6]cyclohepta[1,2-b]pyridine**
24
25 **(22)**

26
27 A mixture of propan-2-one (49 mg, 0.84 mmol), desloratadine (218 mg, 0.70 mmol) and NaBH(OAc)₃ (238
28
29 mg, 1.12 mmol) in DCE (10 mL) was stirred at room temperature for 12 h. The resulting solution was
30
31 diluted with water and extracted with DCM. The organic phase was washed with satd. aq. NaHCO₃
32
33 solution. The organic layer was dried over Na₂SO₄, filtered and concentrated under vacuum. The crude
34
35 mixture was purified by column chromatography (cyclohexane/EtOAc/TEA = 40/58/2, v/v/v) to yield the
36
37 title compound as a pink foam (101 mg, 41% yield).
38
39

40
41 ¹H NMR (500 MHz, CDCl₃) δ 8.39 (dd, *J* = 4.8, 1.7 Hz, 1H), 7.43 (dd, *J* = 7.7, 1.7 Hz, 1H), 7.16 – 7.10 (m, 3H),
42
43 7.08 (dd, *J* = 7.6, 4.8 Hz, 1H), 3.45 – 3.32 (m, 2H), 2.87 – 2.69 (m, 5H), 2.55 – 2.47 (m, 1H), 2.46 – 2.22 (m,
44
45 5H), 1.04 (d, *J* = 6.6 Hz, 3H), 1.03 (d, *J* = 6.6 Hz, 3H). ¹³C NMR (126 MHz, CDCl₃) δ 157.87, 146.76, 139.62,
46
47 137.93, 137.30, 133.55, 132.70, 132.43, 131.08, 129.08, 126.10, 122.17, 54.57, 50.34, 50.19, 32.01, 31.56,
48
49 31.40, 31.13, 18.60, 18.45, one aromatic signal overlapping or not visible. HRMS: C₂₂H₂₆ClN₂ (M+H)⁺ calcd:
50
51 353.1779, found: 353.1770. LC-MS: t_R = 2.9 min, purity >95% (254 nm), m/z: 353.2 (M+H)⁺.
52
53
54
55
56
57
58
59
60

8-chloro-11-(1-ethylpiperidin-4-ylidene)-6,11-dihydro-5H-benzo[5,6]cyclohepta[1,2-b]pyridine (23)

A mixture of acetaldehyde (37 mg, 0.84 mmol), desloratadine (218 mg, 0.70 mmol) and $\text{NaBH}(\text{OAc})_3$ (238 mg, 1.12 mmol) in DCE (10 mL) was stirred at room temperature for 12 h. The resulting solution was diluted with water and extracted with DCM. The organic phase was washed with satd. aq. NaHCO_3 solution. The organic layer was dried over Na_2SO_4 , filtered and concentrated under vacuum. The crude mixture was purified by column chromatography (cyclohexane/EtOAc/TEA = 40/58/2, v/v/v) to yield the title compound as a pink foam (65 mg, 27% yield).

^1H NMR (300 MHz, CDCl_3) δ 8.40 (dd, $J = 4.8, 1.6$ Hz, 1H), 7.43 (dd, $J = 7.7, 1.7$ Hz, 1H), 7.19 – 7.11 (m, 3H), 7.08 (dd, $J = 7.7, 4.8$ Hz, 1H), 3.48 – 3.29 (m, 2H), 2.91 – 2.70 (m, 4H), 2.62 – 2.50 (m, 1H), 2.50 – 2.29 (m, 5H), 2.24 – 2.05 (m, 2H), 1.09 (t, $J = 7.2$ Hz, 3H). ^{13}C NMR (126 MHz, CDCl_3) δ 157.76, 146.78, 139.64, 139.14, 137.93, 137.36, 133.54, 132.75, 132.66, 131.01, 129.08, 126.13, 122.21, 54.65, 54.59, 52.31, 31.97, 31.57, 31.05, 30.79, 12.23. HRMS: $\text{C}_{21}\text{H}_{24}\text{ClN}_2$ ($\text{M}+\text{H}$) $^+$ calcd: 339.1623, found: 339.1608. LC-MS: $t_{\text{R}} = 2.7$ min, purity >97% (254 nm), m/z : 339.1 ($\text{M}+\text{H}$) $^+$.

8-chloro-11-(1-methylpiperidin-4-ylidene)-6,11-dihydro-5H-benzo[5,6]cyclohepta[1,2-b]pyridine fumarate (24)

To a solution of desloratadine (5.00 g, 16.1 mmol) in DCM (150 mL) were added MeOH (75 mL), aq. formaldehyde solution (ca. 13.4 M, 2.40 mL, 32.2 mmol) and AcOH (1.29 mL, 22.5 mmol) and the resulting mixture was stirred at room temperature for 15 min. Subsequently, $\text{NaBH}(\text{OAc})_3$ (5.11 g, 24.1 mmol) was added and the resulting mixture was stirred for 1.5 h at room temperature. The reaction mixture was diluted with 1 M aqueous NaOH (600 mL) and extracted with DCM (2 × 200 mL). The combined organic phases were washed with brine (200 mL), dried over Na_2SO_4 , filtered and concentrated *in vacuo*. Purification by flash column chromatography (DCM/MeOH/TEA 190:5:5) gave the free base (3.96 g) which

1
2
3 was subsequently converted to the fumaric acid salt to obtain the title compound as a white solid (4.27 g,
4
5 60%).

6
7 ^1H NMR (500 MHz, $\text{DMSO-}d_6$) δ 8.36 – 8.32 (m, 1H), 7.57 (d, J = 7.6 Hz, 1H), 7.31 (d, J = 2.0 Hz, 1H), 7.24 –
8
9 7.17 (m, 2H), 7.09 (d, J = 8.2 Hz, 1H), 6.55 (s, 2H), 3.37 – 3.24 (m, 2H), 2.89 – 2.77 (m, 4H), 2.48 – 2.38 (m,
10
11 4H), 2.36 (s, 3H), 2.31 – 2.22 (m, 2H). ^{13}C NMR (126 MHz, $\text{DMSO-}d_6$) δ 167.0, 156.7, 146.4, 140.2, 137.8,
12
13 137.5, 135.3, 134.6, 133.3, 133.2, 131.6, 130.7, 129.0, 125.7, 122.4, 55.1, 44.2, 30.9, 30.6, 29.2, 29.1.
14
15 HRMS: $\text{C}_{20}\text{H}_{22}\text{ClN}_2$ (M+H) $^+$ calcd: 325.1466, found 325.1452. LC-MS: t_R = 2.9 min, purity >99% (254 nm),
16
17 m/z: 324.9 (M+H) $^+$.
18
19
20
21
22

23 **(4-chlorophenyl)(4-iodophenyl)methanol (25)**

24
25 (4-Chlorophenyl)magnesium bromide (1.0 M in Et_2O) (3.23 mL, 3.23 mmol) was added dropwise over 15
26
27 min to a stirred solution of 4-iodobenzaldehyde (500 mg, 2.16 mmol) in Et_2O (4 mL) at 0 °C under nitrogen.
28
29 The mixture was allowed to warm to room temperature and stirred for a further 16 h. Satd. aq. NH_4Cl (1
30
31 mL) was added carefully (**CAUTION!** Exotherm and vigorous bubbling). After bubbling had ceased, the
32
33 mixture was partitioned between Et_2O (10 mL) and satd. aq. NH_4Cl (5 mL). The organic phase was washed
34
35 with brine (5 mL), dried (MgSO_4), filtered and evaporated to give the title compound (655 mg, 88 %) as a
36
37 cream solid.
38
39

40
41 ^1H NMR (400 MHz, CDCl_3) δ 7.59 (d, J = 8.62 Hz, 2H), 7.27 – 7.13 (m, 4H), 7.02 (d, J = 8.36 Hz, 2H), 5.68 (s,
42
43 1H).
44
45
46
47

48 **1-chloro-4-(chloro(4-iodophenyl)methyl)benzene (26)**

49
50 SOCl_2 (0.138 mL, 1.89 mmol) was added dropwise to a stirred solution of **25** (0.65 g, 1.89 mmol) in DCM
51
52 (9.29 mL) at room temperature. After 20 h, the solvent was evaporated under vacuum to give the product
53
54 (0.653 g, 1.799 mmol, 95 %) as a purple solid.
55
56
57

¹H NMR (400 MHz, CDCl₃) δ 7.63 – 7.58 (m, 2H), 7.27 – 7.16 (m, 4H), 7.07 – 7.02 (m, 2H), 5.94 (s, 1H).

2-(4-((4-chlorophenyl)(4-iodophenyl)methyl)piperazin-1-yl)ethanol (27)

A solution of 2-(piperazin-1-yl)ethanol (0.206 g, 1.58 mmol) in toluene (1 mL) was added to **26** (0.637 g, 1.75 mmol) and the mixture was stirred at 80°C under nitrogen for 20 h. The mixture was diluted with DCM and purified by ion exchange chromatography (SCX) eluting with 1 M NH₃/MeOH. Fractions containing product were purified by flash silica chromatography (elution gradient 0 to 5% MeOH-NH₃ (3.5 M) in DCM) to afford the product (165 mg, 0.361 mmol, 21 %) as a white solid.

¹H NMR (600 MHz, DMSO-d₆) 7.65 (d, *J* = 8.1 Hz, 2H), 7.39 (d, *J* = 8.4 Hz, 2H), 7.34 (d, *J* = 8.4 Hz, 2H), 7.20 (d, *J* = 8.2 Hz, 2H), 4.15 (s, 1H), 4.32 (s, 1H), 3.5 – 3.42 (m, 2H), 2.48 – 2.41 (m, 4H), 2.38 (t, *J* = 6.0 Hz, 2H), 2.33 – 2.24 (m, 4H). LCMS (ESI) *m/z* 457.

(S)-2-(2-(4-((4-chlorophenyl)(4-iodophenyl)methyl)piperazin-1-yl)ethoxy)acetic acid (28)

KOH (79 mg, 1.41 mmol) was added to a stirred solution of **27** (161 mg, 0.35 mmol) in DMF (641 μL) at 0°C and the mixture was stirred for 90 min. Sodium 2-chloroacetate (82 mg, 0.70 mmol) was added and the mixture was stirred for 3 h. Water (3 mL) was added and the pH was adjusted to 9 - 10 with aq. HCl (1 M). The mixture was washed with EtOAc (2 x 1 mL) and the pH was adjusted to 4 - 5 with aq. HCl (1 M). The mixture was extracted with DCM (3 x 2 mL). The combined DCM phases were washed with brine (2 mL), dried (MgSO₄), filtered and evaporated to give, after trituration with Et₂O, racemic product (103 mg, 0.200 mmol, 57 %) as an off-white solid.

¹H NMR (600 MHz, DMSO-d₆) 7.69 – 7.65 (m, 2H), 7.44 – 7.4 (m, 2H), 7.38 – 7.34 (m, 2H), 7.22 (d, *J* = 8.4 Hz, 2H), 3.87 (s, 2H), 4.39 (s, 1H), 3.62 (t, *J* = 5.5 Hz, 2H), 2.85 – 2.63 (m, 6H), 2.46 – 2.27 (m, 4H). LCMS (ESI) *m/z* 515.

The stereoisomers were separated by chromatography using a Chiralpak OD column, 5 μm silica, 20 mm

1
2
3 diameter, 250 mm length, eluting with 95/05/0.2/0.1 mixture of MeCN/MeOH/AcOH/TEA to give the
4
5 desired isomer (first eluted) (*S*)-2-(2-(4-((4-chlorophenyl)(4-iodophenyl)methyl)piperazin-1-
6
7 yl)ethoxy)acetic acid (**S**)-28 (7.8 mg)
8
9

11 12 **(R)-5-(4-((4-chlorophenyl)([4-³H]phenyl)methyl)piperazin-1-yl)pentanoic acid ([³H]-Levocetirizine)**

13
14 Precursor (**S**)-28 (0.8 mg, 1.55 μmol), Pd (10% on carbon, 0.5 mg, 0.47 μmol) and Et₃N (5 μL , 0.04 mmol)
15
16 were mixed in EtOH (200 μL). The flask was fitted to the tritium manifold. The mixture was freeze-pump-
17
18 thaw degassed and was then stirred under tritium gas (63.5 GBq) at 162 mbar for 2.5 h. The reaction
19
20 mixture was filtered through a PTFE filter (Whatman 0.45 μm), washing through with more EtOH (5 mL).
21
22 The solution was lyophilised to remove labile tritium, more EtOH (5 mL) was added and the mixture again
23
24 lyophilised. Purification by preparative HPLC (Waters XBridge C18 column, 5 μm , 4.6 x 150 mm) using
25
26 decreasingly polar mixtures of water (containing 0.1% TFA) and MeCN as eluents followed by further
27
28 preparative HPLC (Waters XBridge C18 column, 5 μm , 4.6 x 150 mm), using decreasingly polar mixtures of
29
30 water (containing 0.1% ammonia) and MeCN as eluents, afforded [³H]-levocetirizine (728 MBq) which was
31
32 dissolved in EtOH (10 mL) for storage as a colourless solution.
33
34
35

36
37 Radiochemical purity >98% by HPLC. Chiral purity 93% e.e. by HPLC (obtained on ethyl ester derivative by
38
39 standing in ethanol with TFA for 3 d). LCMS (ESI) *m/z* 391 [M+H]⁺. ³H NMR (640 MHz, DMSO-d₆) 7.20 (t, *J*
40
41 = 7.8). Specific activity by mass spectrometry: 956 GBq mmol⁻¹.
42
43
44
45

46 **Supporting Information**

47
48 Table S1 – Characterization of the kinetics of binding and functional inhibition for H₁R antagonists.

49
50 Figure S1 – Correlations between key physicochemical properties of rupatadine analogs (**1-24**) versus
51
52 the respective pK_i and KRI values at the H₁R.
53

54
55 Table S2 – Physicochemical properties of **1-24**.
56
57

1
2
3 Figure S2 - Figure S3 – Docked binding poses of **1-24** in the H₁R binding pocket.
4

5 Figure S4 - Figure S69 – ¹H-NMR and ¹³C-NMR spectroscopy data as well as high-resolution mass
6 spectroscopy and LC-MS chromatograms.
7

8
9 A CSV file containing the molecular formula strings and associated biochemical data of **1-24**.
10

11 **Corresponding Author Informations**

12
13
14 R. Leurs, r.leurs@vu.nl
15

16 **Present/Current Author Addresses**

17
18
19 A. Kooistra: Department of Drug Design and Pharmacology, University of Copenhagen,
20
21 Universitetsparken 2, 2100 Copenhagen, Denmark.
22

23 M.J. Waring: Northern Institute for Cancer Research, School of Natural and Environmental Sciences,
24
25 Bedson Building, Newcastle University, Newcastle upon Tyne, NE1 7RU, United Kingdom
26

27
28 C. de Graaf: Sosei Heptares, Steinmetz Building, Granta Park, Great Abington, Cambridge CB21 6DG, U.K.
29

30 **Author contributions**

31
32 R. Bosma and Z. Wang have contributed equally to this manuscript.
33

34 **Acknowledgements**

35
36 Hans Custers is acknowledged for technical assistance. This research was financially supported by the
37
38 EU/EFPIA Innovative Medicines Initiative (IMI) Joint Undertaking, K4DD (grant no. 115366) as well as by
39
40 the China Scholarship Council (CSC) (grant no. 201506270163).
41
42

43 **Abbreviations used**

44
45 DCE, dichloroethane; DCM, dichloromethane; DMF, dimethylformamide; DMSO, dimethylsulfoxide;
46
47 GPCR, G protein-coupled receptor; H₁R, histamine H₁ receptor; KRI, kinetic rate index; RecT, recovery
48
49 time; SKR, structure-kinetics relationship; TFA, trifluoroacetic acid; THF, tetrahydrofuran; TEA,
50
51 triethylamine; PSA, polar surface area.
52
53

54 **References**

- 1
2
3 (1) Swinney, D. C. Biochemical mechanisms of drug action: what does it take for success? *Nat. Rev.*
4
5 *Drug Discov.* **2004**, *3* (9), 801–808.
6
- 7 (2) Swinney, D. C. Biochemical mechanisms of new molecular entities (NMEs) approved by United
8
9 States FDA during 2001–2004: mechanisms leading to optimal efficacy and safety. *Curr. Top. Med.*
10
11 *Chem.* **2006**, *6* (5), 461–478.
12
13
- 14 (3) Copeland, R. A.; Pompliano, D. L.; Meek, T. D. Drug-target residence time and its implications for
15
16 lead optimization. *Nat. Rev. Drug Discov.* **2006**, *5* (9), 730–739.
17
- 18 (4) Swinney, D. C. Applications of binding kinetics to drug discovery. *Pharmaceut. Med.* **2008**, *22* (1),
19
20 23–34.
21
22
- 23 (5) Copeland, R. A. The drug–target residence time model: a 10-year retrospective. *Nat. Rev. Drug*
24
25 *Discov.* **2016**, *15* (2), 87–95.
26
27
- 28 (6) Hoffmann, C.; Castro, M.; Rinken, A.; Leurs, R.; Hill, S. J.; Vischer, H. F. Ligand residence time at G-
29
30 protein-coupled receptors-why we should take our time to study it. *Mol. Pharmacol.* **2015**, *88* (3),
31
32 552–560.
33
- 34 (7) Guo, D.; Hillger, J. M.; IJzerman, A. P.; Heitman, L. H. Drug-target residence time-a case for G
35
36 protein-coupled receptors. *Med. Res. Rev.* **2014**, *34* (4), 856–892.
37
38
- 39 (8) Lu, H.; Tonge, P. J. Drug-target residence time: critical information for lead optimization. *Curr.*
40
41 *Opin. Chem. Biol.* **2010**, *14* (4), 467–474.
42
- 43 (9) Vauquelin, G.; Charlton, S. J. Long-lasting target binding and rebinding as mechanisms to prolong
44
45 in vivo drug action. *Br. J. Pharmacol.* **2010**, *161* (3), 488–508.
46
47
- 48 (10) Folmer, R. H. A. Drug target residence time: a misleading concept. *Drug Discov. Today* **2018**, *23*
49
50 (1), 12–16.
51
- 52 (11) Dahl, G.; Akerud, T. Pharmacokinetics and the drug-target residence time concept. *Drug Discov.*
53
54 *Today* **2013**, *18* (15–16), 697–707.
55
56
57

- 1
2
3 (12) de Witte, W. E. A.; Danhof, M.; van der Graaf, P. H.; de Lange, E. C. M. In vivo target residence
4 time and kinetic selectivity: the association rate constant as determinant. *Trends Pharmacol. Sci.*
5
6 **2016**, *37* (10), 831–842.
7
8
9
10 (13) Louizos, C.; Yáñez, J. A.; Forrest, M. L.; Davies, N. M. Understanding the hysteresis loop
11
12 conundrum in pharmacokinetic/pharmacodynamic relationships. *J. Pharm. Pharm. Sci.* **2014**, *17*
13
14 (1), 34–91.
15
16 (14) Vauquelin, G. Effects of target binding kinetics on in vivo drug efficacy: koff, kon and rebinding.
17
18 *Br. J. Pharmacol.* **2016**, *173* (15), 2319–2334.
19
20
21 (15) de Witte, W. E. A.; Vauquelin, G.; van der Graaf, P. H.; de Lange, E. C. M. The influence of drug
22
23 distribution and drug-target binding on target occupancy: the rate-limiting step approximation.
24
25 *Eur. J. Pharm. Sci.* **2017**, *109*, S83–S89.
26
27
28 (16) Santos, R.; Ursu, O.; Gaulton, A.; Bento, A. P.; Donadi, R. S.; Bologa, C. G.; Karlsson, A.; Al-Lazikani,
29
30 B.; Hersey, A.; Oprea, T. I.; Overington, J. P. A comprehensive map of molecular drug targets. *Nat.*
31
32 *Rev. Drug Discov.* **2017**, *16* (1), 19–34.
33
34
35 (17) Simons, F. E. R.; Simons, K. J. Histamine and H1-antihistamines: celebrating a century of progress.
36
37 *J. Allergy Clin. Immunol.* **2011**, *128* (6), 1139–1150.
38
39 (18) Schoepke, N.; Church, M.; Maurer, M. The inhibition by levocetirizine and fexofenadine of the
40
41 histamine-induced wheal and flare response in healthy caucasian and japanese volunteers. *Acta*
42
43 *Derm. Venereol.* **2013**, *93* (3), 286–293.
44
45 (19) Gillard, M.; Van Der Perren, C.; Moguilevsky, N.; Massingham, R.; Chatelain, P. Binding
46
47 characteristics of cetirizine and levocetirizine to human H1 histamine receptors: contribution of
48
49 Lys191 and Thr194. *Mol. Pharmacol.* **2002**, *61* (2), 391–399.
50
51 (20) Church, M. K. Comparative inhibition by bilastine and cetirizine of histamine-induced wheal and
52
53 flare responses in humans. *Inflamm. Res.* **2011**, *60* (12), 1107–1112.
54
55
56
57
58
59
60

- 1
2
3 (21) Church, M. K. Efficacy and tolerability of rupatadine at four times the recommended dose against
4 histamine- and platelet-activating factor-induced flare responses and ex vivo platelet aggregation
5 in healthy males. *Br. J. Dermatol.* **2010**, *163* (6), 1330–1332.
6
7
8
9
10 (22) Sun, C.; Li, Q.; Pan, L.; Liu, B.; Gu, P.; Zhang, J.; Ding, L.; Wu, C. Development of a highly sensitive
11 LC–MS/MS method for simultaneous determination of rupatadine and its two active metabolites
12 in human plasma: application to a clinical pharmacokinetic study. *J. Pharm. Biomed. Anal.* **2015**,
13 *111*, 163–168.
14
15
16
17
18 (23) Solans, A.; Izquierdo, I.; Donado, E.; Antonijoan, R.; Peña, J.; Nadal, T.; Carbó, M.-L.; Merlos, M.;
19 Barbanj, M. Pharmacokinetic and safety profile of rupatadine when coadministered with
20 azithromycin at steady-state levels: a randomized, open-label, two-way, crossover, Phase I study.
21 *Clin. Ther.* **2008**, *30* (9), 1639–1650.
22
23
24
25
26
27 (24) Anthes, J. C.; Gilchrest, H.; Richard, C.; Eckel, S.; Hesk, D.; West, R. E.; Williams, S. M.; Greenfeder,
28 S.; Billah, M.; Kreutner, W.; Egan, R. E. Biochemical characterization of desloratadine, a potent
29 antagonist of the human histamine H1 receptor. *Eur. J. Pharmacol.* **2002**, *449* (3), 229–237.
30
31
32
33 (25) Gillard, M.; Chatelain, P. Changes in pH differently affect the binding properties of histamine H1
34 receptor antagonists. *Eur. J. Pharmacol.* **2006**, *530* (3), 205–214.
35
36
37
38 (26) Bosma, R.; Moritani, R.; Leurs, R.; Vischer, H. F. BRET-based β -arrestin2 recruitment to the
39 histamine H1 receptor for investigating antihistamine binding kinetics. *Pharmacol. Res.* **2016**,
40 *111*, 679–687.
41
42
43
44 (27) Gillard, M.; Strolin Benedetti, M.; Chatelain, P.; Baltes, E. Histamine H1 receptor occupancy and
45 pharmacodynamics of second generation H1-antihistamines. *Inflamm. Res.* **2005**, *54* (9), 367–
46 369.
47
48
49
50
51 (28) Carceller, E.; Merlos, M.; Giral, M.; Balsa, D.; Almansa, C.; Bartroli, J.; Garcia-Rafanell, J.; Forn, J.
52 (3-Pyridylalkyl)piperidylidene]benzocycloheptapyridine Derivatives as Dual Antagonists of PAF
53
54
55
56
57

- 1
2
3 and Histamine. *J. Med. Chem.* **1994**, *37* (17), 2697–2703.
4
5
6 (29) Guo, D.; van Dorp, E. J. H.; Mulder-Krieger, T.; van Veldhoven, J. P. D.; Brussee, J.; Ijzerman, A. P.;
7
8 Heitman, L. H. Dual-point competition association assay: a fast and high-throughput kinetic
9
10 screening method for assessing ligand-receptor binding kinetics. *J. Biomol. Screen.* **2013**, *18* (3),
11
12 309–320.
13
14 (30) Motulsky, H.; Mahan, L. The kinetics of competitive radioligand binding predicted by the law of
15
16 mass action. *Mol. Pharmacol.* **1984**, *25* (1), 1–9.
17
18 (31) Piwinski, J. J.; Wong, J. K.; Green, M. J.; Ganguly, A. K.; Billah, M. M.; West, R. E.; Kreutner, W.
19
20 Dual antagonists of platelet-activating factor and histamine: identification of structural
21
22 requirements for dual activity of N-acyl-4-(5,6-dihydro-11H-benzo[5,6]cyclohepta[1,2-b]pyridin-
23
24 11-ylidene)piperidines. *J. Med. Chem.* **1991**, *34* (1), 457–461.
25
26
27 (32) Zhong, D.; Blume, H. HPLC-determination of loratadine and its active metabolite
28
29 descarboethoxyloratadine in human plasma. *Pharmazie* **1994**, *49* (10), 736–739.
30
31
32 (33) Okada, M.; Hasumi, K.; Nishimoto, T.; Yoshida, M.; Ishitani, K.; Aotsuka, T.; Kanazawa, H.
33
34 Heterocyclic Compound and H1 Receptor Antagonist. US Patent 20130085127, 2013.
35
36
37 (34) Tanoli, S. T.; Ramzan, M.; Hassan, A.; Sadiq, A.; Jan, M. S.; Khan, F. A.; Ullah, F.; Ahmad, H.; Bibi,
38
39 M.; Mahmood, T.; Rashid, U. Design, synthesis and bioevaluation of tricyclic fused ring system as
40
41 dual binding site acetylcholinesterase inhibitors. *Bioorg. Chem.* **2019**, *83*, 336–347.
42
43
44 (35) Baumann, K.; Flohr, A.; Jolidon, S.; Knust, H.; Luebbers, T.; Nettekoven, M. Indol-Amide
45
46 Compounds as Beta-Amyloid Inhibitors. WO Patent 2014060386, 2014.
47
48 (36) Zhang, M. Q.; Leurs, R.; Timmerman, H. Histamine H1-receptor antagonists. *Burger's Med. Chem.*
49
50 *drug Discov.* **1997**, *5*.
51
52 (37) Saxena, M.; Gaur, S.; Prathipati, P.; Saxena, A. K. Synthesis of some substituted
53
54 pyrazinopyridoindoles and 3D QSAR studies along with related compounds: piperazines,
55
56
57
58
59
60

- 1
2
3 piperidines, pyrazinoisoquinolines, and diphenhydramine, and its semi-rigid analogs as
4
5 antihistamines (H1). *Bioorg. Med. Chem.* **2006**, *14* (24), 8249–8258.
- 6
7
8 (38) Tautermann, C. S.; Seeliger, D.; Kriegl, J. M. What can we learn from molecular dynamics
9
10 simulations for GPCR drug design? *Comput. Struct. Biotechnol. J.* **2015**, *13*, 111–121.
- 11
12 (39) Schmidtke, P.; Luque, F. J.; Murray, J. B.; Barril, X. Shielded hydrogen bonds as structural
13
14 determinants of binding kinetics: application in drug design. *J. Am. Chem. Soc.* **2011**, *133* (46),
15
16 18903–18910.
- 17
18 (40) Bortolato, A.; Deflorian, F.; Weiss, D. R.; Mason, J. S. Decoding the role of water dynamics in
19
20 ligand-protein unbinding: CRF1R as a test case. *J. Chem. Inf. Model.* **2015**, *55* (9), 1857–1866.
- 21
22 (41) Kooistra, A. J.; Kuhne, S.; de Esch, I. J. P.; Leurs, R.; de Graaf, C. A structural chemogenomics
23
24 analysis of aminergic GPCRs: lessons for histamine receptor ligand design. *Br. J. Pharmacol.* **2013**,
25
26 *170* (1), 101–126.
- 27
28 (42) Kuhne, S.; Kooistra, A. J.; Bosma, R.; Bortolato, A.; Wijtmans, M.; Vischer, H. F.; Mason, J. S.; de
29
30 Graaf, C.; de Esch, I. J. P.; Leurs, R. Identification of ligand binding hot spots of the histamine H1
31
32 receptor following structure-based fragment optimization. *J. Med. Chem.* **2016**,
33
34 [acs.jmedchem.6b00981](https://doi.org/10.1021/acs.jmedchem.6b00981).
- 35
36 (43) Mocking, T.; Bosma, R.; Rahman, S. N.; Verweij, E. W. E.; McNaught-Flores, D. A.; Vischer, H. F.;
37
38 Leurs, R. Molecular Aspects of Histamine Receptors. In *Histamine Receptors*; Blandina, P.,
39
40 Passani, M. B., Eds.; The Receptors; Humana Press, Cham: Switzerland, 2016; pp 1–49.
- 41
42 (44) Miller, D. C.; Lunn, G.; Jones, P.; Sabnis, Y.; Davies, N. L.; Driscoll, P. Investigation of the effect of
43
44 molecular properties on the binding kinetics of a ligand to its biological target. *Medchemcomm*
45
46 **2012**, *3* (4), 449.
- 47
48 (45) Tresadern, G.; Bartolome, J. M.; Macdonald, G. J.; Langlois, X. Molecular properties affecting fast
49
50 dissociation from the D2 receptor. *Bioorg. Med. Chem.* **2011**, *19* (7), 2231–2241.
- 51
52
53
54
55
56
57
58
59
60

- 1
2
3 (46) Bosma, R.; Witt, G.; Vaas, L. A. I.; Josimovic, I.; Gribbon, P.; Vischer, H. F.; Gul, S.; Leurs, R. The
4 target residence time of antihistamines determines their antagonism of the G protein-coupled
5 histamine H1 receptor. *Front. Pharmacol.* **2017**, *8*, 667–667.
6
7
8
9
10 (47) Shimamura, T.; Shiroishi, M.; Weyand, S.; Tsujimoto, H.; Winter, G.; Katritch, V.; Abagyan, R.;
11 Cherezov, V.; Liu, W.; Han, G. W.; Kobayashi, T.; Stevens, R. C.; Iwata, S. Structure of the human
12 histamine H1 receptor complex with doxepin. *Nature* **2011**, *475* (7354), 65–70.
13
14
15
16 (48) Korb, O.; Stütze, T.; Exner, T. E. Empirical scoring functions for advanced Protein-Ligand docking
17 with PLANTS. *J. Chem. Inf. Model.* **2009**, *49* (1), 84–96.
18
19
20
21 (49) Church, M.; Church, D. Pharmacology of antihistamines. *Indian J. Dermatol.* **2013**, *58* (3), 219–24.
22
23
24 (50) Slack, R.; Russell, L.; Hall, D.; Luttmann, M.; Ford, A.; Saunders, K.; Hodgson, S.; Connor, H.;
25 Browning, C.; Clark, K. Pharmacological characterization of GSK1004723, a novel, long-acting
26 antagonist at histamine H1 and H3 receptors. *Br. J. Pharmacol.* **2011**, *164* (6), 1627–1641.
27
28
29
30 (51) Pan, A. C.; Borhani, D. W.; Dror, R. O.; Shaw, D. E. Molecular determinants of drug-receptor
31 binding kinetics. *Drug Discov. Today* **2013**, *18* (13–14), 667–673.
32
33
34 (52) Tautermann, C. S.; Kiechle, T.; Seeliger, D.; Diehl, S.; Wex, E.; Banholzer, R.; Gantner, F.; Pieper,
35 M. P.; Casarosa, P. Molecular basis for the long duration of action and kinetic selectivity of
36 tiotropium for the muscarinic M3 receptor. *J. Med. Chem.* **2013**, *56* (21), 8746–8756.
37
38
39
40
41 (53) Dowling, M. R.; Charlton, S. J. Quantifying the association and dissociation rates of unlabelled
42 antagonists at the muscarinic M3 receptor. *Br. J. Pharmacol.* **2006**, *148* (7), 927–937.
43
44
45
46 (54) Kuhne, S.; Kooistra, A. J.; Bosma, R.; Bortolato, A.; Wijtmans, M.; Vischer, H. F.; Mason, J. S.; De
47 Graaf, C.; De Esch, I. J. P.; Leurs, R. Identification of ligand binding hot spots of the histamine H1
48 receptor following structure-based fragment optimization. *J. Med. Chem.* **2016**, *59* (19), 9047–
49 9061.
50
51
52
53
54 (55) Baell, J. B.; Holloway, G. A. New substructure filters for removal of pan assay interference
55
56
57

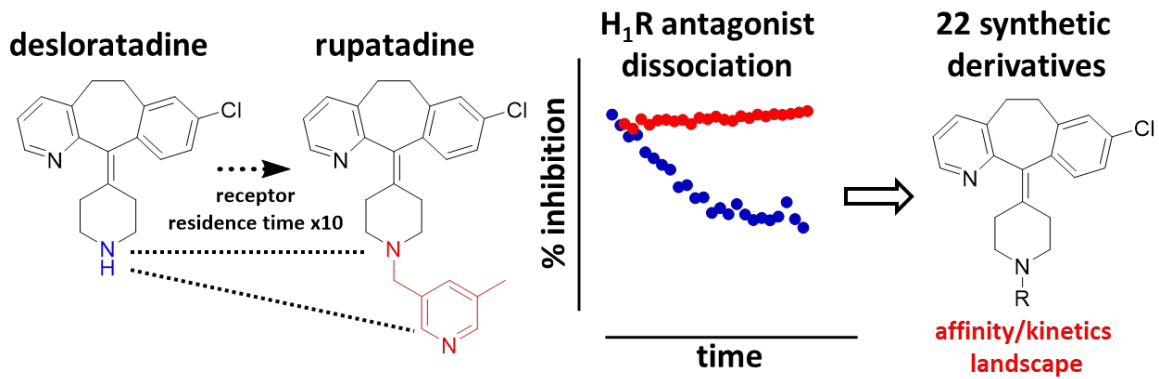
1
2
3 compounds (PAINS) from screening libraries and for their exclusion in bioassays. *J. Med. Chem.*
4
5 **2010**, *53* (7), 2719–2740.

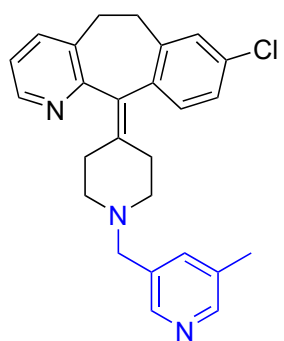
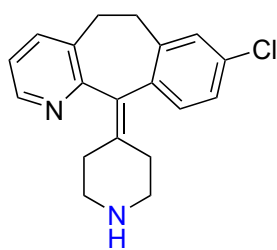
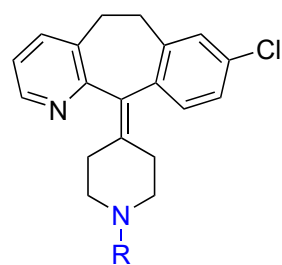
6
7
8 (56) Xie, X.-Q. PAINS-Remover www.cbligand.org/PAINS/ (accessed Mar 10, 2019).

9
10 (57) Cheng, Y.; Prusoff, W. H. Relationship between the inhibition constant (KI) and the concentration
11
12 of inhibitor which causes 50 per cent inhibition (I50) of an enzymatic reaction. *Biochem.*
13
14 *Pharmacol.* **1973**, *22* (23), 3099–3108.

15
16 (58) Marcou, G.; Rognan, D. Optimizing fragment and scaffold docking by use of molecular interaction
17
18 fingerprints. *J. Chem. Inf. Model.* **2007**, *47* (1), 195–207.
19
20
21
22
23
24
25
26
27
28
29
30
31
32
33
34
35
36
37
38
39
40
41
42
43
44
45
46
47
48
49
50
51
52
53
54
55
56
57
58
59
60

Table of Contents graphic



rupatadine, **1**desloratadine, **2**R=alkyl, CH₂-aryl**3-24**

